U.PORTO

FMUP FACULDADE DE MEDICINA UNIVERSIDADE DO PORTO

Pathophysiological role and therapeutic potential of neuregulin-1 in pulmonary arterial hypertension

Pedro Mendes Ferreira

Licenciado em Biologia

TESE DE DISSERTAÇÃO PARA OBTENÇÃO DO GRAU DE MESTRE EM

FISIOPATOLOGIA CARDIOVASCULAR

Orientadora: Professora Carmen Brás Silva

Co-orientador: Professor Doutor Adelino Leite Moreira

PORTO, NOVEMBRO DE 2012

Este trabalho foi desenvolvido no âmbito do projecto financiado pela Fundação para a Ciência e a Tecnologia (FCOMP-01-0124-FEDER-011051, FEDER, COMPETE, Ref. FCT- PTDC/SAU-FCF/100442/2008).

42

(The Hitchhiker's Guide to the Galaxy, 1978)

AGRADECIMENTOS

Ao Professor Doutor Adelino Leite-Moreira por me receber de braços abertos no Departamento de Fisiologia e Cirurgia Cardiotorácica da Faculdade de Medicina da Universidade do Porto, no Mestrado em Fisiopatologia Cardiovascular e no Programa Doutoral em Ciências Cardiovasculares. Um muito obrigado pelo incentivo contínuo e pela disponibilidade em ajudar na formação de um aspirante a cientista.

To Professor Gilles De Keulenaer, for the enthusiastic support throughout the entire work, for sharing your laboratory with me and allowing me to broaden my horizons, and for your very valuable contributions, I would like to thank you.

Ao Professor Doutor André Lourenço pelo extraordinário empenho na minha formação, e pela parte integrante que teve no desenvolvimento da minha capacidade prática e do meu espírito científico. Obrigado por passar de assustador assassino de ratos a amigo. Obrigado pelo exemplo que sempre me deu e pela honestidade com que encarou os meus falhanços e sucessos. Obrigado pelos bons momentos e por me ajudar a ser o pseudo-investigador que hoje sou. O seu espirito crítico e comentários pouco ortodoxos abriram-me os olhos para aquele que é, ao contrário do que achava inicialmente, um mundo dificil e exigente.

À Mestre Maria Mendes José pelas morfo, histo, anatomias dos corações. Obrigado pela paciência e pela disponibilidade. Obrigado por me teres aturado e me receberes sempre com um sorriso na cara. Obrigado por me deixares fazer parte da tua vida e por fazeres parte da minha. Obrigado pela amizade interminável. Fixas-te-te no meu coração.

Ao Dr. Francisco Vasquez-Nóvoa e Rui João Cerqueira pelo apoio nos protocolos experimentais, pelos bons momentos, pelas maratonas investigacionais, e pela boa disposição, obrigado.

Aos meus colegas do Departamento de Fisiologia e Cirurgia Cardiotorácica, o meu muito obrigado por criarem um ambiente tão fácil onde trabalhar. Obrigado pelos sorrisos, pelos “raspanetes” e por me terem aturado durante estes 4 anos. Desculpem a desarrumação, as cantorias e as piadas foleiras, e boa sorte para me aturarem durante mais uns quantos anos. Dulce, Daniela,, Zé Pedro, Marta Pequena, Paulo, Marta Grande, Dona Francelina, Dona Margarida e Dona Rosinha, e todo o corpo docente e não docente do Departamento, agradeço-vos do fundo do coração.

Aos meus amigos, um muito obrigado por me apoiarem independentemente de não saberem o que é uma neuregulina. Obrigado por aturarem os meus deâmbulos científicos e por perceberem que eu não “mato ratos”, mas sim faço experimentação animal. Rita e Vera, o gosto pela ciência está sujeito a discussão, mas a minha adoração por vocês é indiscutível. João, Carlos e Inês, obrigado pelos melhores anos da minha vida. Pelos momentos inesquecíveis e pela amizade incondicional. Um brinde a vocês.

Aos meus pais e irmão, um muito obrigado pela aposta na minha formação profissional e pelo meu crescimento pessoal. Sem vocês não era nada. Pelo apoio interminável e por perceberem que a minha felicidade passa por fazer aquilo que gosto. Obrigado por me deixarem ser feliz.

Aos meus camaradas de armas, Rui Miguel Adão, Carolina Maia Rocha e André Meireles, um muito obrigado pelos bons e maus momentos passados. Pelos sucessos e insucessos, pela força e pela companhia, têm a minha eterna gratidão. Somos os maiores, e não há ninguém à face da terra que prove o contrário.

Finalmente, à minha Orientadora, Professora Carmen Brás Silva, um muito obrigado por tudo. Sinto que não há palavras para lhe agradecer estes 4 fantásticos anos no que é para mim o melhor grupo de investigação do mundo. Obrigado por ter apostado em mim, pela autonomia, pela responsabilidade e pelo apoio. Obrigado por ter recebido um estudante de 2º ano, que não fazia ideia em que se estava a meter, e por me ter tornado um entusiasta da investigação cardiovascular. Obrigado pelas oportunidades, pelas palavras sensatas e por me ter permitido correr meio mundo a espalhar a nossa mensagem. Obrigado pelos sacrificios, pelo apoio nas derrotas e nas vitórias, e acima de tudo pela amizade.

ABSTRACT

Pulmonary arterial hypertension (PAH) is a syndrome based on diverse etiologies and pathogenesis, potentially leading to right ventricular heart failure and death. Neuregulin (NRG)-1 has been implicated in several physiological processes regulating cardiac development, as well as cardiac and vascular homeostasis. Following the notion that NRG-1 has protective effects on the myocardium and vasculature, the question arises whether pharmacological NRG-1/ErbB activation has any therapeutic potential in PAH and ventricular dysfunction. Thus, in this study we investigated the effects of recombinant human (rh) NRG-1 treatment in PAH and its repercussion in myocardial function, in an animal model of monocrotaline (MCT)-induced PAH.

Male Wistar rats randomly received MCT or vehicle. After 14 days, animals were randomly assigned to receive treatment with either rhNRG-1 or vehicle. The study resulted in 4 groups: CTRL, CTRL+rhNRG, MCT and MCT+rhNRG. Echocardiographic, ventricular invasive hemodynamic studies and sample collection for vascular and cardiomyocyte functional studies, as well as for morphometric, histological, and molecular studies were performed 21 to 24 days after MCT administration.

MCT animals developed PAH, demonstrated by impaired pulmonary flow, increased RV systolic pressures and decreased cardiac output. These changes were attenuated with rhNRG-1 treatment. Cardiomyocyte passive tension increase and impaired pulmonary endothelial function and structure, observed in the MCT group, were both reduced in the MCT + rhNRG-1 group.

Administration of MCT resulted in RV hypertrophy, both at the whole heart and at the cardiomyocyte level, concomitant with increased fibrosis. Treating MCT animals with rhNRG-1 decreased overall hypertrophy and fibrosis.

PAH animals presented increased cardiac expression of brain natriuretic peptide and endothelin-1, as well as decreased levels of NRG-1. rhNRG-1 treatment abrogated these changes.

In conclusion, we show that rhNRG-1 treatment is able to restore PAH-induced severe abnormalities in cardiopulmonary function. These findings suggest that the NRG-1 pathway has a relevant role on the pathophysiology of PAH and right ventricular function, representing a potential therapeutic target.

INDEX

Pulmonary hypertension historical perspective

The first case report of what later came up to be primary pulmonary hypertension (PPH), was made in 1891, by Ernst von Romberg. Once he was unable to determine any cause for the abnormalities in the pulmonary vessels observed in patients, he designated these vascular alterations as “pulmonary vascular sclerosis” [1]. “Ayerza’s disease” rose up, in 1901, as the name for PPH and right ventricular failure, and was believed to be caused by syphilis.

During the next four decades, arteritis of the pulmonary arteries caused by syphilis infection continued to be the explanation [2] for the observed vascular abnormalities, until a British histopathologist, Oscar Brenner, in the 1940s, discredited Ayerza’s disease and the etiology proposed for it. He described that PPH was a result of histopathological changes in the small muscular arteries and arterioles [3], although he failed to relate the vasoconstriction associated with arterial remodelling and right ventricular hypertrophy and dilation.

In 1951 the first description of PPH’s pathophysiology arose, when Dresdale and coworkers demonstrated that a patient with PPH presented drastically lowered pulmonary arterial pressures when infused with a systemic vasodilator [4], being later corroborated with a pulmonary-targeted vasodilator [5].

After a surge of pulmonary hypertension (PH), between the late 60’s and early 70’s, associated with the ingestion of aminorex fumarate [6], an appetite suppressant, interest was heightened in the pathophysiology of this disease, leading to a meeting of the World Health Organization (WHO) based on PPH, in 1975, which created the standards for diagnosis, data collection, exploration of new therapies, cooperation between research centres and promotion of public awareness of the disease.

A second WHO meeting (1998) led to the creation of a clinical classification for all diseases associated with PH. In 2003, the classification was re-evaluated and in 2008, the 4th WHO meeting led to the latest classification of PH, defining PAH and non-PAH pulmonary hypertension categories (Table 1).

Table 1. Updated Clinical Classification of Pulmonary Hypertension (Dana Point, 2008)

Pulmonary arterial hypertension (PAH)	Non-PAH pulmonary hyper tension (PH)	
	Well defined cause	Unclear or multifactorial
PAH (1)	Left-heart disease (2)	Unclear/multifactorial mechanisms (5)
Idiopathic	Systolic dysfunction	Haematologic disorders
Hereditary	Diastolic dysfunction	Myeloproliferative disorders, etc.
Drug/toxin induced	Valvular disease	Systemic disorders
Disease associated	Lung diseases/hypoxia (3)	Vasculitis, sarcoidosis, neuro fibromatosis, etc.
CTD	COPD	Metabolic disorders
HIV infection	Interstitial lung disease	Glycogen storage disease , thyroid disorders , etc.
Portal hypertension	Sleep-disordered breathing	Congenital heart disease
Systemic-pulmonary shunts	Chronic exposure to high altitude	(Other than systemic-pulmonary shunt)
Schistosomiasis	Broncho pulmonary dysplasia	Other
Chronic haemolytic anaemia	Developmental abnormalities	Fibrosing mediastinitis , chronic renal failure on dialysis , etc.
Subclass of PAH (1′)	CTEPH (4)	
PVOD and PCH		

Classes are presented between parentheses. CTD - connective tissue disorder; HIV – human immunodeficiency virus; PVOD – pulmonary veno-occlusive disease; PCH - pulmonary capillary angiomatosis; COPD – chronic obstructive pulmonary disease; CTEPH – chronic thromboembolic PH. (adapted from Lourenço, AP et al, 2012 [7])

In Dana Point, the diagnostic criteria were updated and PH is now defined as a mean pulmonary arterial pressure higher than 25 mmHg at rest [8].

PAH pathophisiology

PAH is seriously underdiagnosed, and in spite a couple of population studies estimated the incidence and prevalence of PAH to be 2.4-7.6 cases/million/year and 15-26 cases/million, respectively [9,10], worldwide the numbers would definitely go up, especially with its new association with other pathologies [7]. Besides PAH, non-PAH PH is also taking a more worrisome role since heart failure (HF) is the most frequent cause of PH [7]. Sixty percent of patients with severe left ventricular (LV) dysfunction, as well as 70% of patients with HF with normal ejection fraction (HFNEF) develop PH [11,12]. In 2020, the 3rd cause of death will be COPD, with associated right ventricular (RV) HF [13].

PAH is a syndrome which results in restricted blood flow through the pulmonary arteries, leading to an increase in pulmonary vascular resistances (PVR) and consequently to RVHF. PVR is increased through vascular remodelling, which is caused by excessive cell proliferation and impaired apoptosis, and vasoconstriction, to

a lesser degree [14]. PAH is a panvasculopathy, mainly affecting the small pulmonary resistance arteries, characterized by intimal hyperplasia, medial hypertrophy and arteriolar occlusion [14], in some cases with a genetic component [15-18].

The RV is gaining strength in determining the prognosis [19,20] and risk stratification [21] of PAH patients, and its response to increased afterload determines the patient outcome [22,23]. The RV hypertrophies and dilates due to increased afterload, through elevated PVR, and its adaptive response is irregular amongst different patients. Since the neonatal RV adapts much easier to increased afterload, paediatric PAH, associated with CHD, has a much higher survival rate than adult-developed PH [24]. In spite its established importance in PAH, and the potentially reversible RV hypertrophy and failure [25,26], little is known regarding RV dysfunction and the effects of current therapies on the RV in PAH [7,27].

RV dysfunction in PAH entails neuroendocrine activation, fibrosis, apoptosis, oxidative stress, inflammation and mitochondrial dysfunction [7], and in fact an increase afterload on the RV imposed by elevated PVR is not sufficient in the development of RVHF [28]. PAH-associated ventricular dysfunction does not come one-sided, besides the RV, the LV is also compromised in PH [29], through ventricular interaction and unloading of the LV [30-32].

Current therapies for PAH

Random clinical trials over the past few decades led to the development of several treatment approaches [7]. Currently, accepted treatments for PH comprise calcium channel blockers (CCBs), prostanoids, endothelin receptor antagonists (ERAs) and phosphodiesterase type-5 inhibitors (PDEis) [8].

In the 1980s the focus of PPH treatment was vasodilator drugs [33], which lacked studies regarding their long-term effects. This led to an increased attention being given to high CCBs. However, only a few patients with iPAH responded to therapy with high dosages of CCBs [34]. Due to its negative inotropic effects and systemic vasodilation [35], CCB therapy started being used only when an acute vasodilator test came out positive [36] leading to a decrease in mean pulmonary artery pressure ≥ 10 mmHg reaching a level below 40 mmHg, with a stable or increased cardiac output and sustained systemic pressures [8].

Once vasodilatory and anti-platelet aggregating properties [37] are essential for protection against PH-associated injury [38,39], prostanoids also received interest in the treatment of PH ,. PH patients present decreased pulmonary arteries levels of

prostacyclin synthase [40], as well as urinary levels of prostacyclin metabolites [41], giving a possible explanation for pulmonary vasoconstriction, smooth muscle cell proliferation and increased coagulation [42]. Human trials have demonstrated that prostacyclin treatment resulted in several positive outcomes in patients with PAH [43-49], leading to the approved treatment of PAH with epoprostenol, treprostinil, iloprost and beraprost [7].

Clinical trials have led to the approval of ERAs as treatment for PAH. A non-selective ERA, bosentan led to, in a small cohort study, hemodynamic improvements [50], which persisted in a 1 year follow-up [51]. Larger cohorts also demonstrated improved its efficacy in improving hemodynamic deterioration associated with PAH [52,53]. Despite the beneficial effects of orally-administered bosentan [54], hepatic function deterioration and anemia might occur during treatment [14]. A selective endothelin receptor type A ERA, ambrisentan, has also been approved for the treatment of PAH [55]. Sitaxentan, which has also shown bosentan-like improvements, revealed secondary effects that might induce liver failure [56], leading to its withdrawal from the market [57]. Another non-selective ERA, tezosentan has been getting some attention, specifically in animal models of PAH, where its application resulted in acute attenuation of PAH [58], through improved pulmonary artery pressure and survival [59,60], as well as improved overall hemodynamics and attenuated neuroendocrine activation [61]. Regardless its positive outcomes, and planned clinical trials (NCT01077297), no data is yet available regarding its use in PAH patients.

Nitric oxide (NO), as a selective pulmonary vasodilator, is widely used for the determination of vasoreactivity in patients with PAH [62], and acute treatment of respiratory failure and PH [63]. Cyclic guanosine monophosphate (cGMP) is generated in response to NO, and is degraded by phosphodiesterases (PDE). The usage of PDEis present beneficial effects in PAH. The first used PDEi, sildenafil, improves PH outcome [64,65], showing decreased mean pulmonary artery pressure and PVR [66]. As for sildenafil, another PDEi has been approved for the treatment of PAH, tadalafil [67]

Despite its clear usefulness, possibility of combining different class drugs in a combined therapy [68-70] and promise in preventing the onset of PH, all available therapies only alleviate the symptoms and slow down deterioration, leading to the necessity of invasive procedures, such as lung or lung-heart transplantation, in severe and more advanced cases. Therefore, new strategies for the cure and treatment of PH are needed [71].

Experimental PAH

Several animal models have been used to simulate PH [72]. The chronic hypoxia and monocrotaline injury models are the most commonly used, and regardless the controversial attitude towards the agreement that they do not represent human PAH, they have allowed for a better understanding of PAH and development of novel therapies.

The monocrotaline (MCT)-induced PAH relies on the toxic pyrrolizidine alkaloid present in the plant *Crotalaria spectabilis*, whose ingestion was described to result in progressive development of PH [73]. Upon ingestion, MCT is metabolized in the liver to form a reactive bifunctional cross-linking compound which leads to vascular injury [72]. Its requirement of hepatic metabolization, by cytochrome *P*-450 leads to an increased variability between animals of the same species and strain. The mainly used model is the rat, although other animal models might be exploited [74,75].

The mechanisms through which MCT induces PAH are not fully understood [72], although several studies have determined possible explanations for its pathological action. Muscularization of small sized pulmonary arteries and right ventricular hypertrophy secondary to that [76]. Vascular morphological changes are preceded by adventitial inflammation, involving first intraacinar arteries and,later on, major bronchus associated arteries and the involvement of both arteries and veins [77], which might be regulated by adventitial fibroblasts [78]. Failure of the pulmonary vascular endothelium to repair, through MCT pyrrole-mediated DNA cross-linking [79] might also be underlined on the development of MCT-induced PH. Extracellular matrix alterations are also associated with MCT injury, both at the arterial lumen and at the medial-adventitial border [80]. A more recent study has described that, pulmonary endothelial cells, in response to MCT, present megalocytosis [81], which might contribute to lumen obliteration. These changes in the vascular bed could be the cause for RV modifications, specifically hypertrophy, which might be associated to an imbalance in endothelin-1 synthesis in the pulmonary arteries, contributing to the progression of cardiopulmonary alterations in MCT-induced PAH [82].

In spite of its possible limitations [83], the MCT-induced PAH model has allowed for the development of the most relevant therapeutic approaches to PAH [72], specifically prostanoids and prostacyclin receptor analogs [84-86], ERAs [87-91] and PDEi [92-96].

Recently, a great deal of attention has been given to neuregulin-1 (NRG-1) and its effects in the development and maintenance of the cardiovascular system. This has opened the way for several research groups to determine its effects in treating several

cardiovascular pathologies and to determine the mechanisms through which its cardioprotective action is achieved. Ultimately, this led to clinical trials being approved and the observation that patients with chronic HF treated with NRG-1 showed improved cardiovascular function [97].

To this regard, we believe it might be also implicated in the development and possible treatment of PAH, and therefore, in the next sections of this thesis, we will describe the current knowledge regarding NRG-1 and its possible applications in the treatment of cardiovascular diseases.

Neuregulins and their receptors

Neuregulins are a large family of proteins that are mainly present in the nervous system, heart, mammary glands, intestine and kidneys [98]. It is composed of several members, neuregulins 1 to 4 (NRG-1 to 4). NRG-1s were the first to be described. *Nrg-1* differently transcribed gives rise to three different isoforms, types I to III (Figure 1). These isoforms are classified according to their type specific N-terminal sequence. Type III has a cysteine-rich domain which makes it a transmembrane protein [99]. The EGF-like domain can also form different isoforms, isoform α or β which result from alternative splicing.

Several names have been appointed to the different NRG-1 isoforms: heregulin, Neu differentiating factor (NDF), glial growth factor (GGF I-III), acetylcholine receptor inducing activity (ARIA) and sensory and motor neuron-derived factor (SMDF) [99], and although being the first descriptions in the literature, they do not correlate with each isoforms main biological activity *in vivo* [100].. Functionally, NRG-1 has been the most studied so far. Within the NRG family only NRG-1 has been associated with cardiovascular development and diseased states [98] and thus will be the focus of this review.

NRG-1 proteolytic activation results from the activity of specific proteases, namely beta-secretase 1, a-disintegrin and metalloproteinase (ADAM) domain-containing protein 10, which have different cleavage sites, resulting in different functionally active soluble forms of NRG-1 [101].Both isoforms characteristics and synthesis as transmembrane proteins or non-membrane proteins define their function and biological activity [100].

NRG-1 mRNA expression and protein synthesis is mediated by neurohormones (inhibited by angiotensin II and phenylephrine and induced by endothelin-1), as well as by mechanical strain (which increases NRG-1 expression) [102].

NRGs bind specifically to ErbB receptors, ErbB3 and ErbB4 (also known as HER3 and HER4). Ligand binding activates the specific monomeric receptor and leads to its dimerization. Receptor dimerization results in homodimers or heterodimers which when activated trigger both the mitogen-activated protein kinase (MAPK) and the phosphatidylinositol-3-OH kinase (PI(3)K)/Akt pathways (Figure 2). The activation of this axis is regulated by the combination of receptor dimers and ligand and results in the activation of cell-survival, migration, proliferation, adhesion and differentiation related pathways [100,103]. NRG-1 acts mainly in the nervous system, through ErbB3 receptor and in the heart through ErbB4 receptor activation.

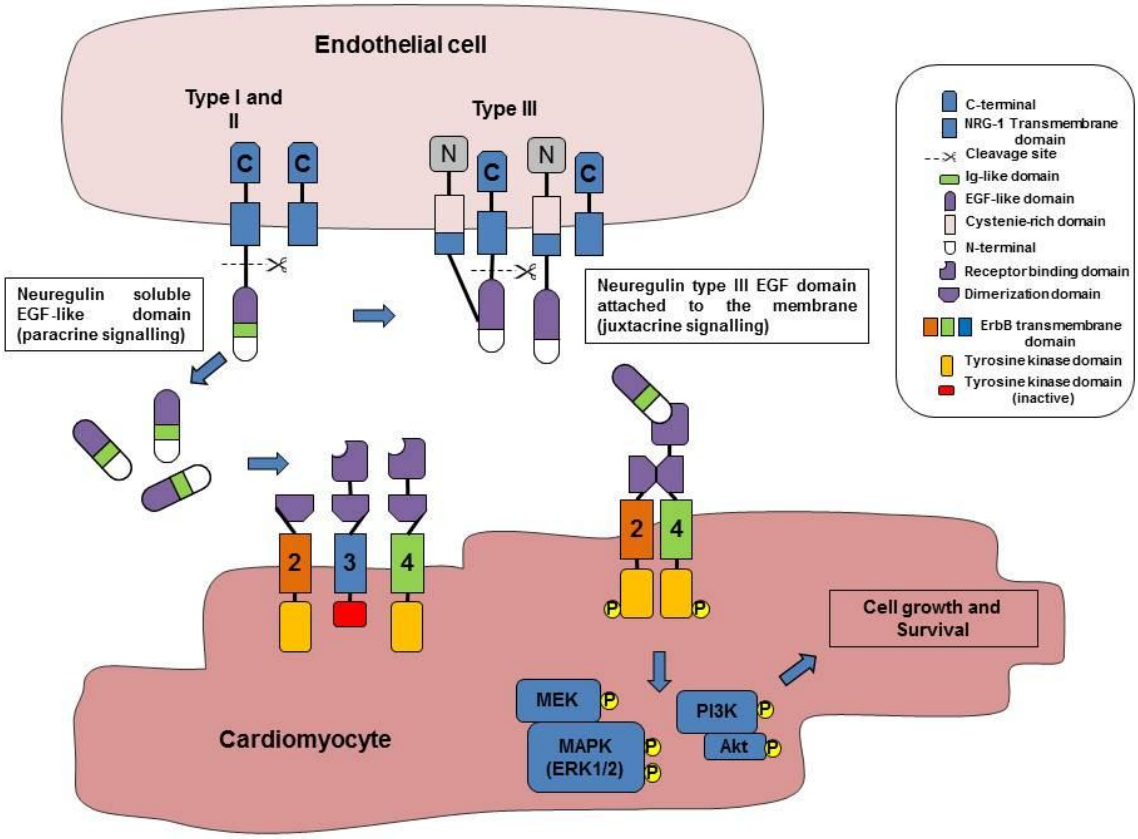

Figure 1 – NRG-1 synthesis and proteolytic activation. NRG-1 can be synthesized either as a soluble form or as a transmembrane form. Types I and II are synthesized as membrane proteins, but upon cleavage by proteases are released in its soluble form and can act in a paracrine way. Type III is synthesized as a two-fold transmembrane protein that upon protease activity is still attached to the membrane, acting in a juxtacrine way. Differences between type I and II are accounted for their EGF-like domain, and while types I and II have an Ig-like domain, type III doesn't. NRG-1 binds to ErbB3 or ErbB4 leading to dimerization of the receptors and transphosphorylation of their tyrosine kinase domains and activation of MEK/MAPK and PI3K/Akt signalling pathways leading to cell growth and survival cascades. ErbB4 is the only receptor who can form active homodimers, since ErbB2 is an "orphan" receptor and therefore cannot be bound by NRG-1 and ErbB3 has an inactive tyrosine kinase domain. Only ErbB2/ErbB4 and ErbB4/ErbB4 dimers are represented, other possible receptor combinations are ErbB2/ErbB3, ErbB3/ErbB4.

NRG-1 role in the cardiovascular system

Besides having a crucial role in cardiac embryonic development and endothelial stem cell differentiation, the NRG-1/ErbB signalling cascade has considerable physiological and pathophysiological functions in the adult heart.

In the heart, NRG-1 is expressed in endocardial and microvasculature endothelium, ErbB4 and ErbB2 are expressed in cardiomyocytes and ErbB3 is expressed in mesenchymal cells of the endocardial cushion [102,104,105]. Ligand and receptors differential expression entails the paracrine transduction pathway associated with this signalling axis, and the presence of different receptors in different cell types determine the different phenotypes observed in differential knock-out models. In fact, *in vitro* studies have confirmed the paracrine way through which NRG-1 acts (specifically, myocardial microvasculature endothelium-synthesised NRG-1 acts on adjacent cardiomyocytes [102]).

NRG-1 role cardiac embryogenesis and cardiac cell differentiation

Several processes in heart embryogenesis are dependent of the NRG-1/ErbB signalling pathway. Cardiac trabeculation and myocardial development is regulated by the NRG-1/ErbB system, which is essential for cardiac muscle differentiation.

ErbB4 mutant mice present deficient myocardial trabeculae formation in the heart ventricle, and die during mid-embryogenesis. The same outcome is present in NRG mutants, demonstrating the direct association between ligand and receptor in the heart and its importance in cardiac development [104,106]. The gene regulatory network required for proper myocardium development is also maintained by this system, in large degree mediated by the transmembrane region of the membrane-anchored NRG-1 [107].

NRGs receptor and co-receptor ErbB3 and ErbB2, respectively, are also important in cardiac development. Heterozygous mice, with a null ErbB2 allele die at an embryonic stage, possibly due to cardiac trabeculae dysfunction [108] and mutant mice lacking the ErbB3 gene present a thinner ventricular wall, and malformation of the cardiac cushion which leads to poor valvulogenesis, resulting in embryo death, as shown for NRG (-/-) and ErbB2 (-/-) mice [109].

Proteolytic activation is also mediated by the intracellular portion, whose mutant impairs ErbB receptor activation [110].

By treating atrioventricular canal explants from mutant (Has2 -/-) mice embryos, which show deficient mesenchymal cell formation, essential for heart valve

development, with NRG-1, a normal phenotype was observed, through phosphorylation of ErbB2 and ErbB3 receptors [111].

Altogether, these studies point to the essential role of NRG-1 signalling in heart embryogenesis.NRG-1 plays a crucial role in cell differentiation in the heart. Depending on the cell type and on the developmental window, it can both lead to the differentiation of cardiac conduction system cells [112], and working type cardiomyocytes [113] .

NRG-1 treatment induces the differentiation of embryonic cardiomyocytes into cardiac conduction system cells, both in cultured cardiomyocytes and in whole embryos [112]. On the other hand, differentiation of stem cells into working type cardiomyocytes is also regulated by NRG-1 [114]. Exogenous administration of NRG-1 further increases the expression of working-type related genes [113]. Conversely, inhibiting NRG-1/ErbB signalling promotes nodal cardiomyocyte formation [113].

NRG-1/ErbB signalling in cardiac cellular responses

Cardiac myocyte apoptosis in response to oxidative stress is regulated by NRG-1. Inhibiting NRG-1/ErbB signalling results in increased cardiomyocyte death, and treating cells with exogenous recombinant NRG-1 promotes cell survival [115]. In the absence of exogenous NRG-1, ErbB4 activation and cellular protection is dependent on the cardiac microvascular endothelial (CMVE)-derived NRG-1β [115]. Cell survival in this context is PI3K/Akt dependent through suppression of mitochondrial cytochrome *c* release and caspase-3 activation [116,117] Furthermore, inhibition of ErbB receptors (4 and 2) leads to induction of Bcl-x splicing towards its pro-apoptotic protein Bcl-xS, leading to mitochondrial dysfunction and apoptosis [118]. Treatment of adult rat ventricular myocyte cultures with NRG-1 resulted in increased proliferation [119], through ErbB4 signalling. Myocyte hypertrophy was also observed, shown by increased protein synthesis and prepro-atrial natriuretic factor upregulation, dependent on the p70S6- and MAPK-kinases [120]. CMVE exerted a cardiomyocyte hypertrophic response, which was abolished by ErbB2 inhibition [102].

NRG-1/ErbB signalling role in cardiac and vascular functionn

Recent experimental evidence reveals that NRG-1 regulates myocardial performance and sympathovagal balance, suggesting that it dynamically participates in hemodynamic homeostasis of the cardiovascular system.

NRG-1 induces a negative inotropic effect, which is preserved during adrenergic stimulation with isoproterenol, providing a counterbalance over the

autonomic imbalance present in heart failure [121]. The negative inotropic effect is dependent on nitric oxide production, through NRG-1 activation of Akt and subsequent eNOS phosphorilation [121].Both eNOS and *β*-adrenoreceptors are translocated to the caveolae, where eNOS attenuates adrenergic stimulation while increasing excitation-contraction coupling. Interestingly, ErbB receptors are also co-localized with eNOS in the caveolae [122], allowing for a better spatial relation between NRG-1 activation of ErbB receptors, and downstream signalling leading to its NO-mediated, anti-adrenergic cardioprotective effects.

Additionally, cardioprotection exerted by parasympathetic muscarinic receptors activation over excessive *β*-adrenergic stimulation, characteristic of heart failure, is abolished in ventricular myocytes from heterozygous (NRG-$1^{+/-}$) mice [123].

Treatment of cardiomyocytes with NRG-1 results in increased cytosolic calcium uptake. Phospholamban is increasingly phosphorylated, in a PI3K and PKG dependent manner, revealing an additional protective role of NRG-1, specifically in diastolic calcium handling [124].

Antagonising ErbB2 while treating cells with a mitotic inhibitor, used in cancer therapy, increases cardiac tissue myofibrilar structural and functional depletion, further confirming the critical role that the ErbB2 receptor plays in protecting the heart from stress induced by chemotherapeutic agents [125].

Growing evidences support a role for NRG-1 in vascular function and structure with clear implications for cardiovascular biology.

NRG-1 is expressed in vascular endothelial cells [126], and its receptors are localized to the underlying smooth muscle cells.

NRG-1 proved to be angiogenic in *in vitro* (collagen gel tube formation) and *in vivo* (rat corneal angiogenesis and chick embryo chorioallantoic membrane) models [127,128].

Undoubtedly, NRG-1's role in angiogenesis is clear, not only in normal physiological conditions, but also in response to tissue damage. In ischemic injury NRG-1 is required for proper angiogenesis and arteriogenesis [129]. Additionally, NRG-1 is expressed in atherosclerotic lesions [130] and associated with the inhibition of neointimal formation and of mitogen-induced vascular smooth muscle cells proliferation and migration after vascular injury [131]. These studies suggest that NRG-1 may be a novel therapeutic candidate for the prevention of neointimal formation in diseases, such as atherosclerosis and restenosis.

NRG-1/ErbB signalling alteration in cardiovascular disease

Together with the premature development of dilated cardiomyopathy in NRG-1/ErbB–deficient mice [132-134], animal studies have demonstrated important changes within the cardiac NRG-1/ErbB system during the progression of heart disease.

NRG-1 mRNA and protein levels, as well as ErbB4 receptor phosphorylation, are increased in response to ischemic damage [135]. Moreover, deleting the NRG-1 gene in endothelial cells causes the abolishment of their cardioprotective role in these conditions. Both at the cell culture and at the whole heart level, endothelial cell-derived NRG-1 has a major protective role against apoptosis and functional impairment during hypoxia/reoxygenation – ischemia/reperfusion, through ErbB4 [136] and eNOS activation [137].

Several studies show that impaired NRG-1 signalling exacerbates the doxorubicin(Dox)-mediated cardiac toxicity. NRG-1, as well as Erbb4 receptor knockouts show increased susceptibility to Dox-treatment [138,139] and Dox-associated cardiomyocyte myofilament injury is increased when NRG-1's co-receptor, ErbB2, is inactivated [140]. Indeed, ErbB2 inhibition and consequent ERK-1 absent phosphorylation is sufficient to abolish CMVE and exogenous NRG-1 protection against anthracycline-induced apoptosis [102]. Moreover, NRG-1 protects against Dox-induced SERCA dysfunction and calcium uptake deficiency through Akt activation [141].

NRG1/ErbB pathway is also impaired in diabetic cardiomyopathy (DCM). Type 2 diabetes in mice leads to deficient ErbB receptor activation in the left ventricle and to delayed cardiac muscle relaxation. Chronic treatment with NRG-1, but not with insulin, reversed these cardiac muscle disturbances [142]. Consistently, ErbB2 and ErbB4 receptor expression and phosphorylation as well as NRG-1 protein synthesis are decreased in DCM [143].

In pacing-induced heart failure, although ErbB2 and ErbB4 receptor phosphorylation increase concurrent with NRG-1 and ADAM19, the downstream signaling is, at least partly, abrogated, once the downstream mediators of the NRG-1/ErbB signalling pathway (Akt and ERK1/2) remained inactivated [144].

In an *in vivo* model of chronic left ventricular hypertrophy secondary to aortic stenosis, both ErbB2 and ErbB4 levels are downregulated when ventricular failure begins [145]. NRG-1 levels were increased during the concentric hypertrophic phase, which correlates with NRG-1 increased synthesis in response to mechanical strain [102]. Upon left ventricular dysfunction and eccentric left ventricular hypertrophy, NRG-1 levels decreased. These changes are possibly due to the increased neurohumoral

activation, mainly mediated by angiotensin II and phenylephrine, during left ventricular failure which exert a negative regulation on NRG-1 production [102].

Collectively, these studies show that in conditions of ventricular damage and dysfunction, activation of NRG1/ErbB signaling is part of an adaptive compensatory program that preserves function. At more advanced stages of ventricular dysfunction, however, activity of the NRG1/ErbB system is attenuated. This maladaptive change is the result of reduced ventricular expression of NRG-1, reduced expression of ErbB receptors, and dysfunctional downstream ErbB signaling. Attenuation of compensatory NRG1/ErbB signaling may thus be an important event in the progression of heart failure.

A graphical representation of NRG-1's effects is presented in Figure 2.

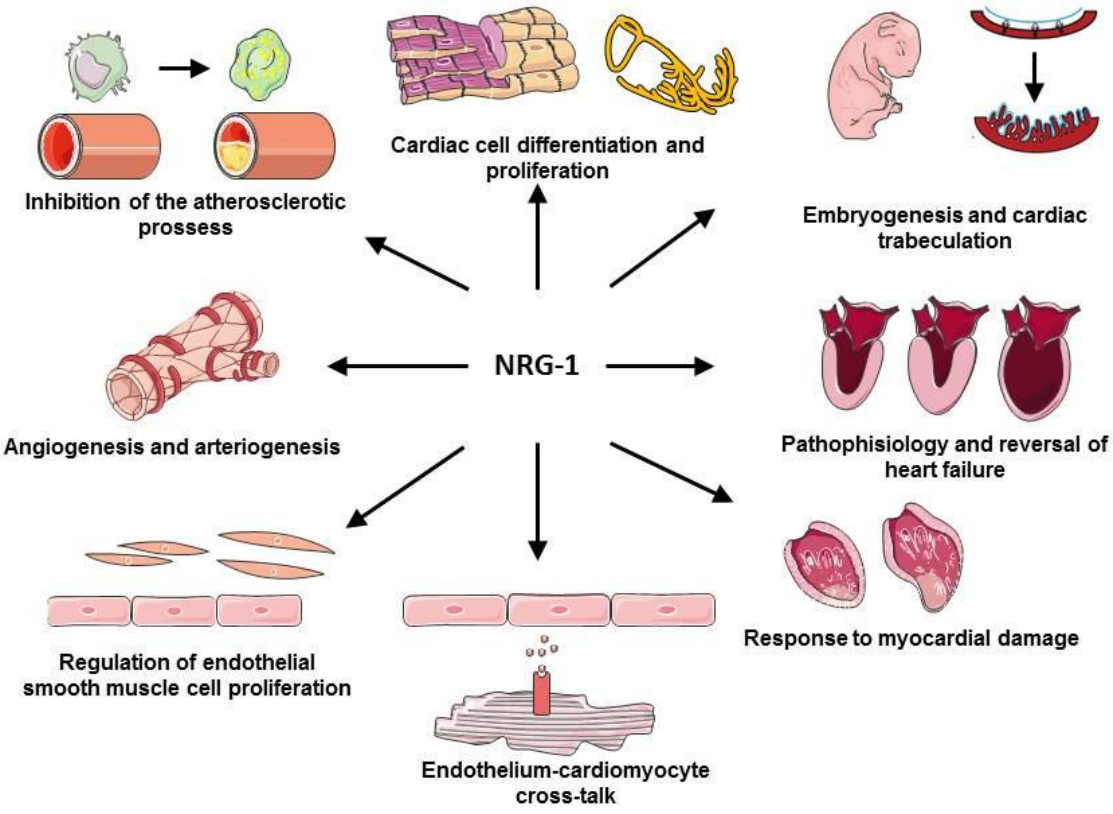

Figure 2 – NRG-1 effects on development and pathophysiology of the cardiovascular system.

Preclinical Studies

The therapeutic potential of NRG-1 as a potential treatment for heart failure has been demonstrated in several animal models models (Table 2).

Structural and functional changes associated with myocardial infarction are attenuated and improved when treatment with NRG-1 is applied [119,146,147], and this effect is dependent on PI3K/Akt activation [135,146,148]. This improvement in function is partially related with the cardiomyocyte replacement after ischemic injury [119]. Additionally, transfection of myocardial infarct areas with lentivirus carrying an overexpressed NRG-1 gene, resulted in improved cardiac function and prevention of apoptosis [149].

In Dox-induced cardiomyopathy, treatment with NRG-1 improved cardiac function and survival [147,150].

Treating DCM-induced rats with NRG-1 resulted in improved ventricular function and structure. Left ventricular systolic and diastolic dysfunction associated with diabetes were significantly attenuated, as well as apoptosis and fibrosis of the heart tissue [151] .

In *in vivo* and in vitro myocarditis models, NRG-1 treatment attenuated the impairment of cardiac function, as well as, protected against histological and biochemical (decreased plasmatic cTnI levels) changes [147].

NRG-1 administration produced global improvements in cardiac performance in a canine model of pacing-induced heart failure [147]. Additionally, in primates, namely rhesus monkeys, with pacing induced heart failure, NRG-1 treatment enhanced contractility (through alpha-myosin heavy chain upregulation), and protected against apoptotic injury [152].

Altogether, these results suggest that the NRG-1/ErbB signalling pathway is in fact altered in cardiac injury and modulation of this axis results in improved cardiac function.

Table 2 – Neuregulin-1 therapeutic effects in animal models of heart failure.

Ref.	Model / species	Treatment	Outcome
[147]	MI / rat	10 μg/kg/day IV. for 5 or 10 days 1 week or 2 months after LAD ligation	Improved LV structure and function, decreased neurohumoral activation and improved survival.
[119]	MI/mouse	2.5 ug/mouse IP for 12 weeks 1 week after LAD	Improved structure and function
[135]	MI – I/R /rat	1, 2, 4 or 8 μg/kg IV for 20 minutes prior to I/R	Improved structure, decreased release of ischemia-injury markers and decreased apoptosis
[148]	MI/ rat	5 μg/kg/h IV for 7 days, 8 weeks after LAD ligation	Improved structure and function through MLC upregulation
[146]	MI /rat	10 μg/kg/d IV for 10 days, 4 weeks after LAD ligation	Improved structure and function and attenuation of mitochondrial dysfunction
[149]	MI /rat	Injection of infarcted area with rhNRG-1 carrying lentivirus	Decreased apoptosis and increased revascularization through increased Akt and eNOS activation
[147]	Dox-induced CM / rat	20 μg/kg/day IV for 5 days 4 weeks after first doxorubicin administration	Improved function and survival, and decreased necrosis
[150]	Dox-induced CM	0.75 mg/kg/day SC for 3-5 days (beginning 1 day prior to doxorubicin administration)	Improved function and survival, decreased myocardial injury markers and increased Akt phosphorylation
[153]	DCM / rat	Inhibitory anti-ErbB4 30 μg, IV 3 times per week for 4 weeks	Decreased NRG-1/ErbB signaling and pro-inflammatory gene expression, while no changes in LV function
[151]	DCM / rat	10 μg/kg, IV every 2 days, for 2 weeks, 12 weeks after streptozotocin injection	Improved LV function and decreased apoptosis and fibrosis
[147]	Myocarditis / mouse	30 μg/kg/day IV for 5 days	Improved LV structure and function and survival, and decreased myocardial necrosis
[147]	CRP / beagle dog	3 μg/kg/day IV for 5 days with continuous pacing, 3 weeks after after the beginning of rapid pacing	Improved function
[152]	CRP / rhesus monkey	3 μg/kg/day IV for 10 days	Improved function and increasedα MHC expression

Akt – protein kinase B; CM – cardiomyopathy; CRP – chronic rapid pacing; DCM – diabetic cardiomyopathy; Dox – doxorubicin; eNOS – endothelial nitric oxide synthase; IP – intraperiotneal IV – intravenous; I/R – isquemia/reperfusion; LAD – left anterior descending artery; LV – left ventricular; MI – myocardial infarction; MHC – myosin heavy chain; MLC – myosin light chain; SC – subcutaneous.

Human studies

Since the observation that patients undergoing clinical trials for cancer treatment with trastuzumab, an antagonist of the ErbB2 receptor, developed an increased risk of cardiac dysfunction, huge attention was given to the NRG-1/ErbB pathway in the heart [154]. Animal research has demonstrated the importance of the NRG-1/ErbB pathway in cardiac development and its pathophysiology, leading to several experimental studies that tried to characterize its function and determine its role in human cardiovascular function.

Several “bench” studies have taken the data gathered so far and with human samples have tried to describe through which mechanisms NRG-1 is involved in human cardiovascular disease.

In ventricular tissue from patients with advanced heart failure, increased NRG-1 and decreased ErbB2/ErbB4 mRNA expression have been observed. Interestingly, in patients who had left ventricular unloading with ventricular assist devices, the changes reversed [155].

Quantification of serum NRG-1 levels, in a cohort of 899 patients with chronic heart failure, showed that increased NRG-1 levels were associated with increased disease severity (I-IV class of the New York Heart Association - NYHA) and risk of death or cardiac transplantation. This study identifies NRG-1 as a novel biomarker of heart failure, presenting a higher correlation together with brain natriuretic peptide than each biomarker individually [156].

Patients with coronary artery disease, namely acute coronary syndrome and effort angina pectoris presented lower plasmatic levels of NRG-1 than patients with mild hypertension or healthy subjects. The lowest levels of NRG-1 detected in acute coronary syndrome patients inversely correlated with the severity of lesions. In addition, NRG-1 expression (by macrophage foam cells) was found to be directly correlated with the progression of the atherosclerotic plaque [157]. Another group demonstrated that both serum and plasma NRG-1 levels inversely correlated with severity of coronary artery disease. In this study plasma NRG-1levels were two-fold higher than serum and were higher in patients with stress-induced ischemia [158].

Perik et al [159] in a cohort of 50 heart failure patients found that serum ErbB2 was increased in patients with higher NYHA classes, lower left ventricular ejection fraction and higher apoptotic-related cytokines. However, a larger cohort of 765 showed that plasmatic levels of ErbB2 were not associated with left ventricular end-diastolic pressure or ejection fraction, in spite myocardial tissue deregulation of HER2 expression [160].

Clinical trials

Recent clinical trials have demonstrated the effects of the therapeutic administration of recombinant human NRG-1 (rhNRG-1) in patients with stable chronic heart failure on optimal medical therapy [161,162] (Table 3).

A phase II trial, in which a daily intravenous infusion of rhNRG-1was given to patients during 10 consecutive days, showed an increase in left ventricular function and structure observed at day 30 after the 10-day treatment. On day 90, structure and function were even further increased [161].

Another phase II trial in which patients received a consecutive 12 hour intravenous infusion of rhNRG-1 during 10 days showed an increase in cardiac output of 30% and a decrease in pulmonary artery wedge pressure and systemic vascular resistance of 30 and 20%, respectively. Twelve weeks following the 11 days infusion left ventricular ejection fraction suffered a 12% increase [162].

Importantly, in these studies, the short-term rhNRG-1 administration was safe and well tolerated.

Larger trials are now on-going. A phase IIa interventional clinical trial, has set to determine, over a period of 12 months, the efficacy and safety of NRG-1 as a treatment in 120 patients with chronic heart failure(NCT01251406), and the same group also planned a phase III clinical trial with the purpose of evaluating the efficacy of NRG-1 in reducing death rate of this condition(NCT01541202).

Table 3 – rhNRG-1 clinical trials

Ref	Description	Patients	Dosage	End-Points	Outcomes
[161]	Phase II, randomized, double-blind, multicenter, background therapy-based, placebo-controlled, parallel group study	44	0.3, 0.6 or 1.2 μg/kg 10-h IV infusion for 10 consecutive days	Change in LVEF%, ESV or EDV as measured by MRI at baseline and days 11, 30 and 90 Cardiac function classification (NYHA); 6-min walk test; QOLS; Plasma NT-proBNP.	Improved and sustained LVEF% and decreased LVEDV and LVESV at 30 and 90 days after treatment compared with baseline (no differences between the treated and placebo group)
[162]	Single-centre, prospective, non-randomized, open label study	15	Initial dose of 1.2 μg/kg for 6 h 0.6, 1.2 or 2.4 μg/kg 12 hour IV infusion for 10 consecutive days	Changes in acute (first 24 h) and sustained after 12 weeks haemodynamics measured by Swan-Ganz catheterization; Changes in LVEDV, LVESV and LVEF measured by MRI on days 12, 28 and 84; Changes in NA, ALD, ET-1, NT-proBNP, PIIINP, highly sensitive hsCRP, TNF-α and IL-6.	Acute increase in CO; Improvement in LVEF; No changes in LVEDV or LVM; Decrease of serum NA and aldosterone.

ALD – aldosterone; CO – cardiac output; EDV – end-diastolic volume; ESV – end-systolic volume; ET-1 – endothelin-1; hsCRP – highly sensitive C-reactive protein; IL-6 – interleukin-6; LVEF – left ventricle ejection fraction; LVM – left ventricle mass; MRI – magnetic resonance imaging; NA – noradrenaline; NT-proBNP – n-terminal pro-B-type natriuretic peptide; NYHA – new york heart association; PIIINP – procollagen III N-terminal propeptide; QOLS – quality of life score;TNF-α – tumor necrosis factor alpha.

Purpose

Animal research data has allowed the determination of several effects and subcellular mechanisms through which NRG-1 acts on cardiovascular system, in health an disease, leading to several studies in human patients.

Results from clinical trials have proved that indeed NRG-1 is a modulator of cardiovascular function, showing improvements in several hemodynamic parameters in patients with chronic heart failure, both acutely and in a long time period manner, underlying its important role in the cardiovascular system and its potential usage as a HF therapeutic agent.

Following the notion that NRG-1/ErbB signaling has protective effects on the myocardium and vasculature, the question arises whether pharmacological NRG-1/ErbB activation has any preventive or curative potential in PAH and RV heart failure..

Taking into account that RV failure is the most severe complication of PAH, and NRG-1's effect in improving cardiac function and structure in several animal models, leads us to assume that NRG-1 might result in an attenuation of RV deterioration in PAH.

The structural changes seen in the pulmonary vessels in PAH include medial thickening (due to smooth muscle cell hyperplasia and hypertrophy), formation of a neointimal composed of smooth muscle cells or myofibroblasts embedded in a mucopolysaccharide matrix and the occurrence of plexiform lesions (due to endothelial and smooth muscle cell proliferation). To date, there are no studies concerning the effect of NRG-1/ErbB system in pulmonary vasculature, but we know that NRG-1 is synthesised by the endothelium, its receptors are expressed in the underlying smooth muscle cells, and additionally, that NRG-1 attenuates neointimal formation following vascular injury, and inhibits the proliferation of vascular smooth muscle cells in other vascular beds (7), facts that emphasize the need of experimental studies in order to determine the role of NRG-1/ErbB system in PAH context.

One of the most successful therapeutic approaches to PAH has been ET-1 blockade through bosentan, an orally active nonselective ET receptor antagonist, approved by the Food and Drug Administration. Recently, ET-1 involvement in the LV dysfunction that accompanies longstanding severe PAH, has been shown [163]. Moreover, it is also known that endothelial NRG-1 synthesis is stimulated by ET-1 [102]. On the other hand, there is experimental evidence showing the existence of an inhibitory cross-talk between ET and ErbB receptors in the adult heart [164]. These facts reinforce once more the pertinence of the present study, having into account the

relevance of the ET-1 system for the pathophysiology of PAH and RV HF and its interaction with the NRG-1 system.

We therefore believe that NRG-1 might play a pivot role in the pathophysiology and treatment of PAH and PAH-associated RV hypertrophy and failure. To this point we set out to determine the effects of rhNRG-1 chronic treatment in an animal model of MCT-induced PAH.

Based on the actual knowledge described in the previous sections, we hypothesize that activating the NRG-1 system in PAH animals might protect not only lung vessels, but also the RV and LV myocardium and thus increase animal survival, attenuate PAH and improve RV and LV myocardial function. Therefore, this work aimed to investigate the role of the NRG-1/ErbB system in the pathophysiology PAH and in the progression to HF and, thus, to contribute for the development of new therapeutic approaches.

Our specific goals are: (i) to determine changes in the expression of NRG-1 in the heart tissue from healthy rats and from rats with PAH induced by MCT; (ii)to assess changes in RV and LV myocardial function and the severity of PAH, in vivo (hemodynamic and echocardiographic studies) and in vitro (isolated cardiomyocytes and pulmonary vascular muscle studies); (iii) to analyze myocardial and pulmonary structure and histology, and their patterns of gene expression in healthy animals and in animals with PAH with or without short-term NRG-1 treatment.

The work plan was executed in the context of the funded project "Role of the neuregulin system in pulmonary arterial hypertension - pathophysiological and therapeutic implications" (ref.PTDC/SAU-FCF/100442/2008).

METHODS

All the procedures in this work followed the recommendations of the Guide for the Care and Use of Laboratory Animals, published by the US National Institutes of Health (NIH Publication No. 85-23, Revised 1996), and are accredited by the Portuguese Direção Geral de Veterinária (DGV) and approved by Fundação para a Ciência e a Tecnologia (FCT PTDC/SAU-FCT/100442/2008).

Animal model

Seven week-old male Wistar rats (Charles River Laboratories, Barcelona, Spain) weighing 180–200g, were randomly assigned to receive either a subcutaneous injection of 60mg/kg monocrotaline (MCT, Sigma Chemical) or an equal volume of vehicle (saline). Fourteen days after MCT/vehicle administration, animals were randomly assigned into 4 subgroups: (i) untreated animals (CTRL); (ii) animals with induced PAH and without pharmacological treatment (MCT); (iii) animals with induced PAH and with pharmacological treatment (MCT + rhNRG-1); (iv) animals without PAH and with pharmacological treatment (CTRL + rhNRG-1). Pharmacological treatment consisted on a daily intraperitoneal administration of 40μg/kg of rhNRG-1 (Peprotech, Offenbach, Germany) during 7 days, while the vehicle treatment consisted in Bovine Serum Albumin (BSA, Sigma-Aldrich, 0.1% during 7 days). A separate group was created, where MCT animals received a 250mg/kg/d gavage of bosentan (25mg/mL in 5% gum Arabic, starting 2 days after MCT or vehicle, kindly provided by Actelion Pharmaceuticals).The drug dosages, administration routes, and treatments duration were selected on the basis of previous studies from our and others research teams [119,147,163,165] or of preliminary dose-finding studies (unpublished data).

Animals were grouped 5 per box, in a controlled environment, with a light-darkness cycle of 12:12h, controlled temperature at 22ºC, and water and food *ad libitum*. Before MCT administration, an echocardiographic evaluation was performed, in order to allow a basal evaluation to compare experimental groups and also as a guarantee that the potentially ill animals (with cardiac disease or other) did not follow the protocol. Between 21 and 24 days after MCT administration, the animals were submitted again to an echocardiographic evaluation and to invasive hemodynamic evaluation. After invasive heamodynamic evaluation, samples were collected and processed for *in vitro* functional studies in cardiomyocytes and pulmonary arteries, as well as for morphometric, histologic and molecular biology studies.

Echocardiography studies

Echocardiographic studies were performed one day before the administration of MCT (or vehicle) and 21 to 24 days after MCT (or vehicle) injection.

Animals were anesthetized by an intraperitoneal injection of ketamine/xylazine (75mg/kg and 10mg/kg, respectively), placed in left lateral decubitus and the skin was shaved. After applying warm echocardiography gel, a 12MHz sensorial probe (GE Healthcare) was gently placed on the thorax.

Acquisitions (General Electrics Vivid 7 echocardiograph, GE Healthcare) were averaged from three consecutive heartbeats. Bi-dimensional and M-mode images were obtained, in short axis of LV at the papillary muscle level. End-systolic and end-diastolic LV diameter and wall size were evaluated. In apical projection of 4 and 5 cavities, after previous acquisition of bi-dimensional image, tricuspid valve flow and pulmonary valve flow, were evaluated by conventional Doppler. Right atria area was evaluated in the 4 chamber view and tricuspid annular plane systolic excursion in M-mode following alignment of the gate to the tricuspid valve.

Invasive haemodynamic evaluation

As previously described [166], 21 to 24 days after MCT administration, anesthesia was induced by an intraperitoneal injection of fentanyl and midazolam (100 µg/kg and 5 mg/kg, respectively) and inhalation of 8% sevoflurane (Penlon Sigma Delta). Endotracheal intubation was performed using a 14 gauge catheter and mechanical ventilation controlled by a rodent ventilator (MouseVent G500, Kent Scientific, Connecticut, USA). Anesthesia was maintained with sevofluorane (2.5-3.0% vol/vol). The internal femoral vein was catheterized (24G) under surgical microdissection (Wilde M651, Leica microsystems, Cambridge, UK) for infusion (Multi-Phaser, NE-100, New Era Pump Systems) of warm lactate Ringer's solution at a rate of 8 mL/Kg/h. Animals were placed in right-lateral decubitus and after tricotomy, a left thoracotomy was performed. Pericardium and pleura were carefully dissected, and the phrenic nerve was severed. A 3-0 surgical silk was passed around the inferior vena cava (IVC) for transient occlusion during the protocol, and pressure-volume catheters were inserted through the apex of RV and positioned along the long axis (PVR-1045, 1F, Millar Instruments). A flow probe was implanted around the ascending aorta (MA2.5PSB, 2.5mm, Precision S-Series, Transonic Systems). The experimental preparation was allowed to stabilize for 15 minutes. Baseline and IVC occlusions recordings were obtained with ventilation suspended at end-expiration. Pressure and volume signals were continuously acquired (MVPS 300, Millar instruments), digitally

recorded at a sampling rate of 1000Hz (ML880 PowerLab 16/30, ADinstruments), and analyzed off-line (PVAN 3.5 Millar Instruments). Parallel conductance for the volume catheter was computed (PVAN) after bolus injection of 50µL hypertonic saline (10%), calibration for factor alpha (field inhomogeneity) was determined through the cardiac output calculated through the aortic flow probe and the ultrasonic transit time volume flowmeter (TS420, transit-time perivascular flowmeter, Transonic systems).

Following an intravenous 100 mg/kg pentobarbital injection, animals were exsanguinated and heparinized blood was collected and used for volume calibration with standard cuvettes (P/N 910-1048, Millar Instruments).

Samples of RV and lung tissue were collected and snap frozen in liquid nitrogen and stored at -80ºC. For mRNA quantification, samples were submerged in RNA stabilization reagent (RNAlater, Qiagen, 76106, Crawley, UK) and for histological analysis samples were stored in buffered 10% formaldehyde.

***In vitro* studies in isolated skinned cardiomyocytes**

Frozen VD tissue samples were collected in a Petri dish filled with relax solution (5.89 mM Na_2ATP, 6.48 mM MgCl2, 40.76 mM Propionic acid, 100 mM BES, 6.97 mM EGTA and 14.5 mM Creatinine phosphate) and were cut in small pieces. Tissue was then pottered to 2.5 mL of relax solution and submitted 3 times to mechanical homogenization for 3 seconds at 30 rpm (High Speed 4000 rpm homogenizer, Glas-Col, Terre Haute, Indiana, USA). Fresh relax solution (2.5 mL) and 0.5 mL of Triton 10% were added, making a final volume of 5.5 mL. The previous procedures were performed on ice. Solution was then left at room temperature for 5 minutes, in order to allow Triton to permeabilize cells and dissolve cardiomyocytes' membranes. Homogenate was washed 5 times with relax solution in spin-down cycles of 1 minute, 1500rpm, and 4ºC (between each wash, lid was removed and a new one was added to prevent Triton contamination).

After isolation, cells were placed under the inverted microscope (IX51 inverted microscope, Olympus) and one single cardiomyocyte was attached to the transducer and motor tips (1600A – Permeabilized Myocyte Test System, Aurora Scientific), with the help of commercial silicone, at a temperature of 20ºC. After 25 minutes to allow a proper attachment of the cell to the setup (Model 803B Permeabilized Myocyte Test Aparatus, Aurora Scientific), the tests were performed.Cell length was adjusted between 2.0 and 2.3 µm and recorded by the motor (315C High-Speed Length Controller, Aurora Scientific), which was controlled via computer using custom-designed software (Series 600A Digital Controller, Aurora Scientific). For offline

analysis, force development was also recorded by computer (Series 400A Force Transducer Systems, Aurora Scientific). The developed force was measured during each activating cycle, being the zero force level identified by instituting a quick ramp shortening in cell length, just before moving the cell back to relaxing solution. Force development was measured by varying submaximal free-Ca2+ concentrations (using a stock solution of 5.97 mM Na_2ATP, 6.28 mM $MgCl_2$, 40.64 propionic acid, 100 mM BES, 7 mM CaEGTA and 14.5 mM creatinine phosphate) in between the test contractions, and corrected for rundown by assuming that each contraction between the test contractions at maximum activation contributes equally to the force rundown.

The pCa ranged from 9.0 (relax solution) to 4.5 (maximal activation) (to the proportion of the several Ca2+ solutions. Maximal activation was used in the calculation of maximal Ca2+-activated isometric force (Fmax), and the exposure to solutions with intermediates pCa yielded the force-pCa relation, normalized for cross-sectional area. Once a steady-state force level was reached, the cell was shortened within 1ms to 80% of the original length (slack test) and after 20ms the cell was re-stretched and returned to the relaxing solution, in which another slack test (duration of 10 seconds) was performed.

Active tension is given as the difference between total tension, measured by slacking the preparation during the steady activation (distance between the baseline of the force transducer and the steady-force level), and passive tension, measured by slackening the relaxed preparation.

Cells were not included in final analysis if force declined more than 20% between the second and the last test contraction at maximum activation [167].

***In vitro* studies in vascular preparations**

Following previously described methodology [168], 21 to 24 days after MCT/vehicle injection animals were euthanized with 100 mg/kg sodium pentobarbital (Eutasil, CEVA). Lungs and heart were excised *en bloc* and the left upper lobe was used to carefully isolate 2nd generation pulmonary artery (200 – 400 μm diameter) under the stereo microscope (Stemi 2000C Stereo Microscope, Zeiss). Arterial rings were isolated (2 ± 0.2 mm) and mounted between two metallic pins in a horizontal bath myograph system (DMT Myograph 720 MO, ADInstruments). Throughout the isolation and protocol, the tissue was submerged in modified Krebs-Ringer solution (130 mM NaCl, 4.7 KCl, 1.18 mM KH_2PO_4, 1.17 mM $MgSO_4$, 14.9 mM $NaHCO_3$, 5.5 mM glucose, 0.026 mM EDTA and 1.6 mM $CaCl_2$), at a constant temperature of 37ºC, 95% O_2/5% CO_2 and pH 7.4. After a stabilization period, a length-tension curve was

obtained through progressive stretching of the arterial rings (20% increase intervals) until the target transmural pressure was achieved (target transmural pressure was obtained through right heart catheterization as previously described). The preparations were allowed to stabilize at target transmural pressure and stimulated with 80 mM KCl solution to determine maximum tension development. Three to four solution changes followed in order to relax the arterial rings and endothelial function was evaluated through a dose-response curve to acetylcholine (10^{-9} to 10^{-5} M, in 0.5 logarithmic units intervals) performed on pre-contracted rings (10^{-5} M phenylephrine). Analysis was performed offline using appropriate software (LabChart 7 Pro, ADInstruments).

Histological and morphometric studies

Immediately after exsanguination of the anesthetized/instrumented animal, heart and lungs were excised and weighted [169]. RV and LV + septum were carefully dissected and weighted separately. Tissue weight was normalized to animal bodyweight. Heart failure is associated with cachexia [166,170] and therefore, normalizing tissue weights of MCT-injected animals might lead to an overestimate of cardiac hypertrophy. In order to eliminate bodyweight as a factor in tissue weight normalization, tibial length, which remains constant throughout adulthood, was measured and served as a normalizer [171].

Samples for histology were submersed in a fixative solution of 10% formaldehyde. After the initial fixation step, samples underwent dehydration (using ethanol in decreasing percentages), diaphanisation (using xylene) and impregnation in liquid paraffin (54 ° C). Later they were placed and properly oriented in metal molds, and serial sections of 4 μm and 3 μm were obtained from RV and pulmonary arteries, respectively, in a Minot type microtome.

Haematoxylin and eosin (HE) stained sections of RV were digitally photographed (Olympus XC30 Digital colour Camera) and cardiomyocyte cross-sectional area and diameter were measured using imaging software (cell^B, Olympus). Fifty muscle fibers per animal were analyzed and only nuclei-centered cardiomyocytes were considered for analysis.

Sirius Red staining, which stains collagen fibers, was used to determine fibrosis on RV sections. Digital images were analyzed using image analysis software (Image-Pro Plus version 6.0, Media Cybernetics Inc.). Seven randomly selected fields were analyzed per animal by two blinded observers.

Van Gieson staining, which distinguishes smooth muscle from collagen fibers, was used to determine the area and thickness of pulmonary artery sections. Images were acquired and analyzed as previously mentioned.

Molecular studies

Total mRNA from cardiac tissue samples was extracted after homogenization in a metal mortar (~800 rpm rotor), through the guanidinium thiocyanate silica-gel membrane-binding method according to the manufacturer's instructions (Quiagen 74124) [163,172],. Sample purity (as assessed by the 260/280 nm absorption ratio) and total mRNA concentration were assayed by spectrophotometry (Eppendorf 6131000.012). Two-Step real-time RT-PCR was used for relative mRNA quantification. For each studied gene, standard curves were generated based on the correlation between the quantity of starting total mRNA and the PCR threshold cycle (second derivate method) of successive dilutions of a random rat cardiac tissue sample ($r \geq 0,98$). Equal amounts of total mRNA from every sample (50 ng) underwent three separate two-step real time RT-PCR experiments with specific primers for each gene. RT was performed using a standard thermocycler (Whatman Biometra 050-901), in a total volume of 20μL, with 40U/reaction of reverse transcriptase (invitrogen 18064-014), 20U/reaction of RNase inhibitor (Promega N2515), 30ng/mL random primers (invitrogen 48190-011), 0,5mM nucleotide mix (MBI Fermentas R0192), 1,9mM $MgCl_2$, and 10mM DTT, at 22°C, 50°C and the 95°C, for 10, 50, and 10 minutes, respectively. PCR was performed with 2μL cDNA as template in a total volume of 20μL (LightCycler II®, Roche), using hot-start polymerase and SYBR green as marker (Quiagen 204143) according to the manufacter's instructions. Melting curve analysis of each PCR reaction was performed to exclude primer-dimer formation and to assess the purity of the amplification product.

The results of mRNA quantification are expressed in arbitrary units (AU), the mean of CTRL group after normalization for GAPDH corresponding to 1 AU. The primer pairs used to quantify genes were: GAPDH – P1-5'TGGCCTTCCGTGTTCCTACCC3', P2-5'CCGCCTGCTTCACCACCTTCT3'; NRG-1 – P15'AAGCTGGCCATTACGTAGTTTTG3', P2-5'TGTGCGGAGAAGGAGAAAAACTTTC3'; ET-1 - P15'CGGGGCTCTGTAGTCAATGTG3', P2-5'CCATGCAGAAAGGCGAATGTC3'; BNP - P15'CAGAGCTGGGGAAAGAAGAG3', P2-5'GGACCAAGGCCCTACAAAAGA3'.

Statistical analysis

Statistical analysis was performed using *GraphPad Software* (vs.5). 2-way ANOVA was used to statiscally analyse all the presented parameters, except endothelial function which underwent a 2-way repeated measures ANOVA test. Holm-Sidak's method was performed for post hoc comparisons between groups. Group data are presented as means±SEM and were compared using two-way ANOVA. Differences with $p<0,05$ were considered statistically significant.

RESULTS

Echocardiographic evaluation

The full echocardiographic analysis is presented in Table 4. MCT-treated animals developed RV hypertrophy, as indirectly measured by 2-dimentional M-mode analysis of the interventricular septum thickness (IVSDD), while no statistically significant changes occurred in the LV free wall thickness. Left ventricle end diastolic diameter (LVEDD) was decreased in the MCT group. Treatment with rhNRG-1 resulted in reversal of RV remodeling, although LVEDD was not significantly reverted.

Doppler imaging analysis revealed a deficit on the right heart flow. Pulmonary flow was altered in the pulmonary hypertensive animals, as shown by the decreased pulmonary flow velocity (PAPSV), acceleration time (PAAT) and velocity time integral (PAVTI) when compared with healthy animals. The ratio PAAT/ejection time (PAET) was also altered in the MCT group. Treatment with rhNRG-1 restored velocity and acceleration time of blood flow in the pulmonary artery, normalizing the PAAT/PAET ratio.

Transvalvular flow analysis revealed the presence of both pulmonary and tricuspid regurgitation associated with pulmonary hypertension, where MCT animals presented reverse flow through both the tricuspid (2.530 ± 0.608 *vs*. 0.609 ± 0.059, MCT *vs.* CTRL) and pulmonary valves (0.888 ± 0.288 m/sec, no reverse flow was detected in other groups besides MCT). Treatment with rhNRG-1 decreased tricuspid incapacity and eliminated pulmonary insufficiency.

Right atria area was also increased in MCT animals and a tendency was observed in the tricuspid annular plane systolic excursion (TAPSE) to be increased in the same group. Pharmacological rhNRG-1 intervention also normalized both these parameters.

Table 4 – Echocardiographic evaluation

	CTRL		MCT	
	vehicle	**rhNRG-1**	**vehicle**	**rhNRG-1**
LVPWDD (mm)	1.40 ± 0.07	1.41 ± 0.08	1.49 ± 0.11	1.31 ± 0.11
LVEDD (mm)	6.93 ± 0.10	6.86 ± 0.20	5.87 ± 0.43*	6.41 ± 0.12
IVSDD (mm)	1.478 ± 0.097	1.633 ± 0.078	2.150 ± 0.141*	1.667 ± 0.119$^{\#}$
LVEF (%)	86.48 ± 1.25	87.99 ± 1.88	89.43 ± 2.41	89.57 ± 1.63
APSV (m/s)	0.98 ± 0.04	0.97 ± 0.07	0.80 ± 0.04*	0.86 ± 0.02$^{*\#}$
PAPSV (m/s)	1.06 ± 0.04	1.08 ± 0.02	0.87 ± 0.04*	0.98 ± 0.02$^{\#}$
PAAT (ms)	28.74 ± 1.28	28.55 ± 0.91	19.41 ± 2.17*	25.48 ± 1.79$^{\#}$
PAAT/PAET	0.32 ± 0.01	0.31 ± 0.01	0.21 ± 0.03*	0.27 ± 0.04$^{\#}$
PAVTI	6.04 ± 0.23	6.29 ± 0.17	4.43 ± 0.48*	5.61 ± 0.19$^{\#}$
RVEDD (mm)	5.00 ± 0.07	5.10 ± 0.23	5.32 ± 0.21	5.00 ± 0.20
RAA (cm^2)	0.13 ± 0.02	0.12 ± 0.01	0.22 ± 0.02*	0.14 ± 0.01$^{\#}$
TAPSE (cm)	0.18 ± 0.01	0.17 ± 0.03	0.22 ± 0.02	0.18 ± 0.03

APSV – aortic peak systolic velocity; LVEF – left ventricle ejection fraction; SF – shortening fraction; IVSDD – interventricular septum diastolic diameter; LVEDD – left ventricle end diastolic diameter; LVPWDD – left ventricle posterior wall diastolic diameter; PAAT – pulmonary artery acceleration time; PAAT/PAET – pulmonary acceleration time / pulmonary artery ejection time; PAPSV – pulmonary artery peak systolic velocity; PAVTI – pulmonary artery velocity time integral; RAA – right atria area; RVEDD – right ventricle end diastolic diameter; TAPSE – tricuspid annular plane systolic excursion. $^{*}p < 0.05$ vs CTRL + vehicle; $^{\#}p < 0.05$ vs MCT + vehicle.

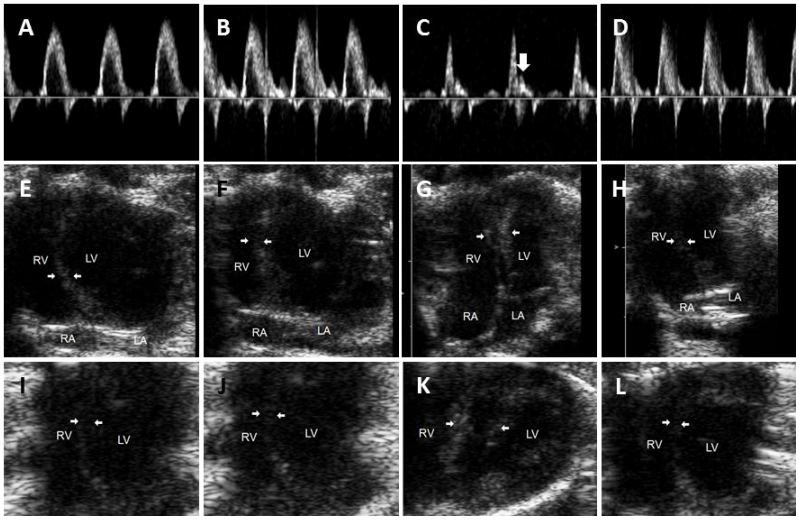

Figure 3 – Transthoracic echocardiographic analysis. Representative images from the CTRL + vehicle (**A,E,I**), CTRL + rhNRG-1 (**B,F,J**), MCT + vehicle (**C,G,K**) and MCT + rhNRG-1 (**D,H,L**) groups showing the pulmonary flow pattern (**A-D**), apical 4-chamber view (**E-H**) and parasternal short-axis view (**I-L**). In the apical 4-chamber and parasternal short-axis view white arrows represent the interventricular spetum. MCT + vehicle animals reveal the presence of a midsystolic notch (white arrow in image **C**) and a deviation of the IVS to the left side of the heart (white arrows in images **E-L**). Treatment with rhNRG-1 restored both pulmonary waveform (**D**) and IVS structure (**H** and **L**).

Invasive hemodynamic evaluation

Heart catheterization evaluation showed that several parameters of both systolic and diastolic function were altered in MCT animals (Table 5). Both end-systolic and end-diastolic RV pressures increased, and cardiac output was compromised in pulmonary hypertensive animals. Pharmacological rhNRG-1 treatment significantly improved all the above mentioned parameters.

MCT-injected animals revealed impaired diastolic function, both by compromised relaxation, as measured by dP/dt_{min}, and increased RV stiffness, as measured by the end-diastolic pressure volume relationship (k1). Systolic function was improvedas shown by the increased RV contractility, as measured by dP/dt_{max}, and the by end systolic pressure volume relationship ($slope_{(Emax)}$). rhNRG-1 treatment led to an attenuation of both diastolic dysfunction and increased inotropy that were observed in the MCT group.

Considering the LV, systolic pressures were decreased in the MCT group and diastolic dysfunction was also evident, as revealed by the decrease in the $-dP/dt_{min}$ and the increase in the isovolumic relaxation time. Treating rats with rhNRG-1 increased maximum developed pressures and improved diastolic function.

Table 5 – Left Ventricle and Right ventricle hemodynamic evaluation

	CTRL		MCT	
RV	**vehicle**	**rhNRG-1**	**vehicle**	**rhNRG-1**
$P_{máx}$ (mmHg)	32.9 ± 2.3	34.0 ± 2.1	58.8 ± 4.0*	49.0 ± 3.6$^{*\#}$
CO (mL.min^{-1})	64.3 ± 17.2	62.0 ± 6.8	40.0 ± 18.7*	53.7 ± 9.0$^{*\#}$
EDP (mmHg)	2.26 ± 1.29	2.38 ± 0.37	4.66 ± 3.94*	2.47 ± 1.29$^{\#}$
dP/dt_{max} (mmHg.s^{-1})	2262 ± 134	2301 ± 152	3519 ± 205*	2917 ± 199$^{\#}$
$-dP/dt_{min}$ (mmHg.s^{-1})	2199 ± 145	1760 ± 107	3050 ± 195*	2484 ± 246$^{\#}$
LV				
P_{max} (mmHg)	126.1 ± 3.4	118.6 ± 4.5	96.2 ± 5.9*	104.5 ± 4.8$^{*\#}$
$-dP/dt_{min}$ (mmHg.s^{-1})	10267 ± 626	9207 ± 404	4762 ± 585*	6823 ± 972$^{*\#}$
τ (ms)	8.27 ± 0.50	7.99 ± 0.15	10.77 ± 0.72*	9.14 ± 0.55$^{\#}$
	IVC occlusions			
RVESPVR (linear)				
Slope (E_{max}), (mmHg.µL^{-1})	0.14 ± 0.04	0.17 ± 0.09	0.9 ± 0.28*	0.29 ± 0.05$^{*\#}$
RVEDPVR (exponential)				
k_1	0.006 ± 0.004	0.005 ± 0.001	0.019 ± 0.005*	0.008 ± 0.001$^{\#}$
dP/dt_{max}–EDV (mmHg .s^{-1} .µL^{-1})	9.97 ± 2.41	10.12 ± 5.32	28.29 ± 6.08*	16.57 ± 5.77$^{\#}$
LVEDPVR (exponential)				
k_1	0.01 ± 0.00	0.01 ± 0.00	0.03 ± 0.01	0.01 ± 0.00

Left (LV) and Right Ventricular (RV) hemodynamic evaluation of control vehicle treated (CTRL + vehicle), control treated with recombinant human NRG-1 (CTRL + NRG-1), monocrotaline-injected treated with vehicle (MCT + vehicle) and monocrotaline-injected treated with recombinant human NRG-1 (MCT + NRG-1) rats. CO - cardiac output; $dP/dt_{min/max}$ minimum and maximum rate of pressure change; EDP - end-diastolic pressure; EDPVR – end-disatolic pressure volume relationship. ESPVR - end-systolic pressure-volume relationship; Pmax – maximum pressure; τ - time constant of isovolumetric relaxation; $^{*}p < 0.05$ vs. CTRL + Vehicle and $^{\#}p < 0.05$ vs. MCT + vehicle.

In vitro studies in isolated skinned cardiomyocytes

The analysis of the total force development showed that MCT group isolated RV cardiomyocytes were able to develop higher force than the CTRL group cells (17.71 ± 5.83 *vs*. 13.85 ± 3.96 N/m^2, MCT *vs*. CTRL) (Figure 4-A). In cardiomyocytes from

rhNRG-1 treated rats' total developed force was significantly lower than in the MCT group cells and similar to CTRL group cardiomyocytes (12.59 ± 3.15 N/m^2).

MCT-group isolated cardiomyocytes developed higher passive force when compared to CTRL group cells, at the sarcomere lengths of 2.0 (1.76 ± 0.26 *vs*. 1.43 ± 0.29 N/m^2, MCT *vs*. CTRL), 2.2 (3.74 ± 0.71 *vs.* 2.68 ± 0.24 N/m^2, MCT *vs*. CTRL), and 2.3 µm (5.73 ± 1.22 *vs*. 3.86 ± 0.87 N/m^2, MCT *vs*. CTRL). Treatment with rhNRG-1 was able to significantly restore the passive force development to levels similar to the CTRL group cardiomyocytes (1.28 ± 0.25, 3.04 ± 0.55, and 3.63 ± 0.89 N/m^2, at 2.0, 2.2, and 2.3 µm respectively). The CTRL + rhNRG-group cardiomyocytes developed significantly less passive force when compared to CTRL group cells (1.19 ± 0.25, 2.32 ± 0.55, and 3.16 ± 0.54 N/m^2, at 2.0, 2.2, and 2.3 µm, respectively) as represented in Figure 4-B.

Active force was also increased in cardiomyocytes from MCT animals when compared to controls (14.39 ± 1.47 *vs*. 11.10 ± 0.41 N/m^2, MCT *vs* CTRL), rhNRG-1 chronic treatment resulted in no differences from healthy animals (9.67 ± 0.67 N/m^2) as represented in Figure 4-C.

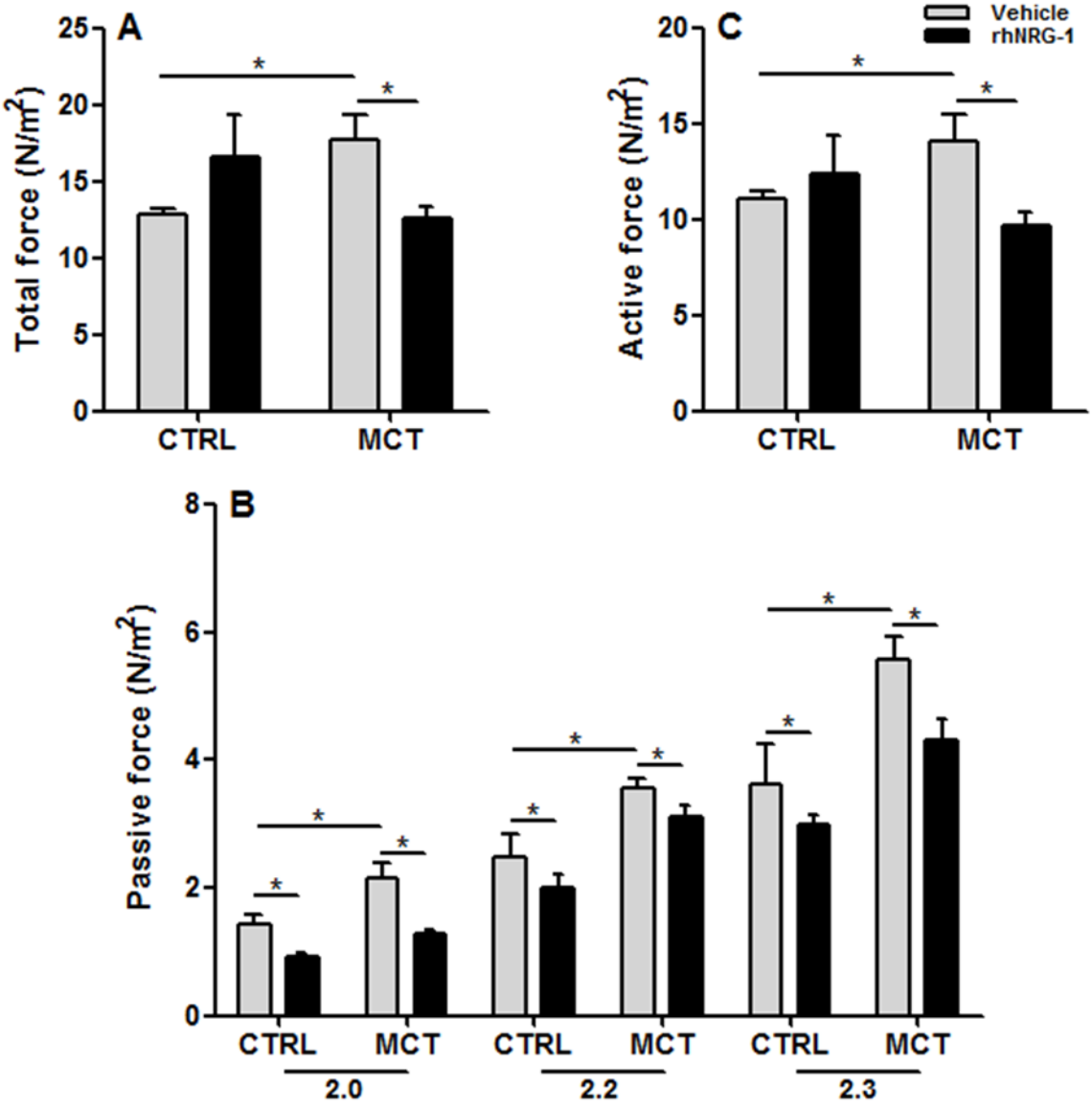

Figure 4 – Permeabilized isolated cardiomyocyte force development. MCT group animals showed higher levels of total force development (**A**) when compared to the CTRL group. Passive force evaluated at 2.0, 2.2 and 2.3 mm of sarcomeric length (**B**) showed increased development of passive force in the MCT group. Active force development was higher in the MCT group when compared to the CTRL group (**C**). MCT + rhNRG-1 animals showed no differences from the CTRL group in total, passive and active force. * $p < 0.05$ in line-targeted groups.

In vitro studies in vascular preparations

Endothelial dysfunction, due to MCT-induced pulmonary hypertension was present in MCT animals, as shown by the impaired relaxation of pulmonary arterial rings to increasing doses of acetylcholine (35.41 ± 4.02 *vs*. 86.27 ± 1.85 %, MCT *vs*. CTRL), with significant increase of the EC50 ($6.69x10^{-7}$ ± $1.41x10^{-7}$ *vs*. $1.95x10^{-7}$ ±

3.93x10^{-8} M, MCT *vs*. CTRL). Pulmonary rings from rhNRG-1 treated animals showed improved endothelial function (48.31 ± 5.67 % and 2.45x10^{-7} ± 6.30x10^{-8} M) when compared to untreated pulmonary hypertensive animals (Figure 5).

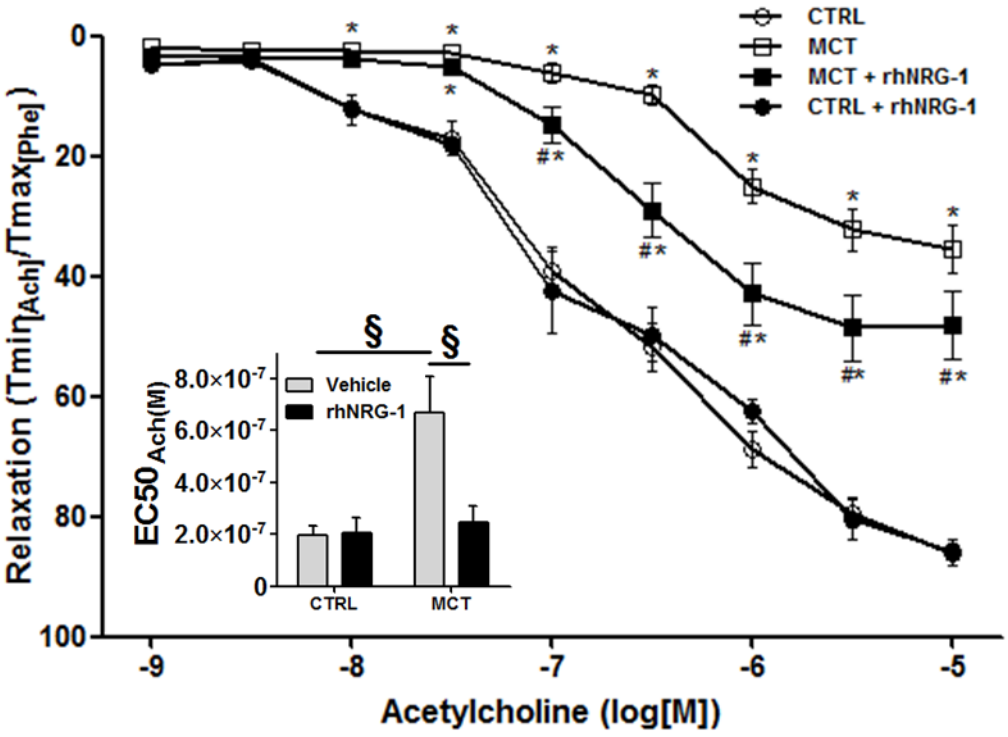

Figure 5 – Pulmonary arterial endothelial function evaluation. Pre-contracted arterial ring (10^{-5} M phenylephrine) submitted to acetylcholine (10^{-9} to 10^{-5}M) showed decreased relaxation in the MCT group when compared to the CTRL group. MCT + rhNRG-1 animals showed improved relaxation when compared to the MCT group. EC50 was increased in the MCT animals, while treatment with rhNRG-1 normalized the EC50 value. * $p < 0.05$ *vs*. CTRL + vehicle; $^{\#}$ $p < 0.05$ *vs*. MCT + vehicle, § $p < 0.05$ in line-targeted groups.

Morphometric and histological analysis

Induction of pulmonary hypertension gave rise to heart hypertrophy (4.26 ± 0.14 *vs*. 3.10 ± 0.06 g/kg, MCT *vs*. CTRL) which was accounted to RV hypertrophy with an increase in the RV weight / body weight ratio (1.21 ± 0.03 *vs.* 0.55 ± 0.02 g/kg, MCT *vs*. CTRL), RV weight / tibia length ratio (0.076 ± 0.002 *vs*. 0.045 ± 0.001 g/cm, MCT vs. CTRL) and RV weight / LV + Septum ratio (0.53 ± 0.02 *vs*. 0.27 ± 0.01 g/kg, MCT *vs*. CTRL). Lung weight was also increased (0.742 ± 0.034 *vs*. 0.436 ± 0.021 g/cm, MCT *vs*. CTRL) in pulmonary hypertensive animals. Gastrocnemius liver weight showed no differences between groups. rhNRG treated animals presented decreased ventricular remodeling (0.057 ± 0.003 g/cm) and lung weight (0.618 ± 0.036 g/cm) as presented in Table 6.

Table 6 – Morphometrical analysis

	CTRL		MCT	
	vehicle	**rhNRG-1**	**Vehicle**	**rhNRG-1**
HW/BW (g/kg)	3.10 ± 0.06	3.12 ± 0.06	4.26 ± 0.14*	3.43 ± 0.11$^{\#}$
RVW/BW (g/kg)	0.55 ± 0.02	0.58 ± 0.83	1.21 ± 0.03*	0.83 ± 0.06$^{*\#}$
RVW/LV+SW (g/g)	0.27 ± 0.01	0.29 ± 0.01	0.53 ± 0.02*	0.40 ± 0.02$^{*\#}$
RVW/TL (g/mm)	0.05 ± 0.00	0.05 ± 0.00	0.08 ± 0.00*	0.06 ± 0.00$^{*\#}$
LW/TL (g/mm)	0.44 ± 0.02	0.41 ± 0.01	0.74 ± 0.03*	0.62 ± 0.04$^{*\#}$
LiW/TL	2.58 ± 0.08	2.59 ± 0.17	2.29 ± 0.13	2.58 ± 0.11
GcW/TL	51.49 ± 1.56	49.92 ± 2.44	44.69 ± 1.45	45.78 ± 1.44

BW – body weight; GcW – gastrocnemius; HW – heart weight; LiW – liver weight; LV+SW – left ventricle + septum weight; LW – lung weight; RVW – right ventricle weight; TL – tibia length; $^{*}p < 0.05$ vs CTRL + vehicle; $^{\#}p < 0.05$ vs MCT + vehicle.

RV remodeling was further confirmed by increased cardiomyocyte cross sectional area and diameter (536.67 ± 59.46 mm^2 and 25.35 ± 1.19 mm *vs*. 375.39 ± 47.43 mm^2 and 20.84 ± 1.02 mm, MCT *vs*. CTRL, respectively) in diseased animals, while rhNRG treatment decreased cardiomyocyte hypertrophy (409.01 ± 19.72 mm^2 and 22.18 ± 0.61 mm) as represented in Figures 6-7.

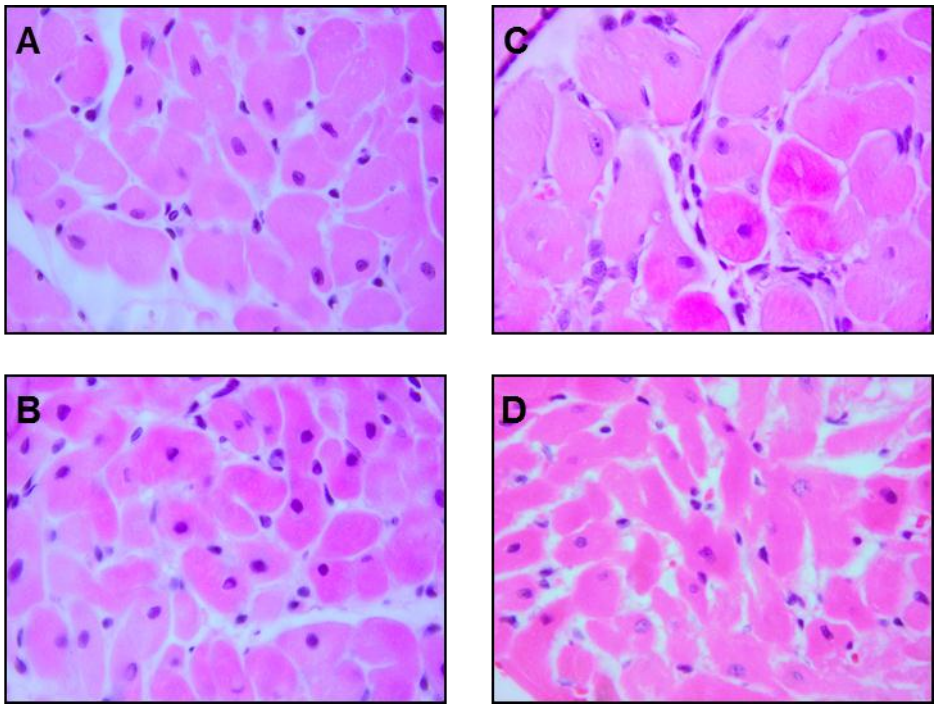

Figure 6 - Histological analysis of cardiomyocyte structure. Light microscopy images of hematoxylin-eosin stained sections of RV (400x) from CTRL + vehicle (**A**), CTRL + rhNRG-1 (**B**), MCT + vehicle (**C**) and MCT + rhNRG-1 (**D**).

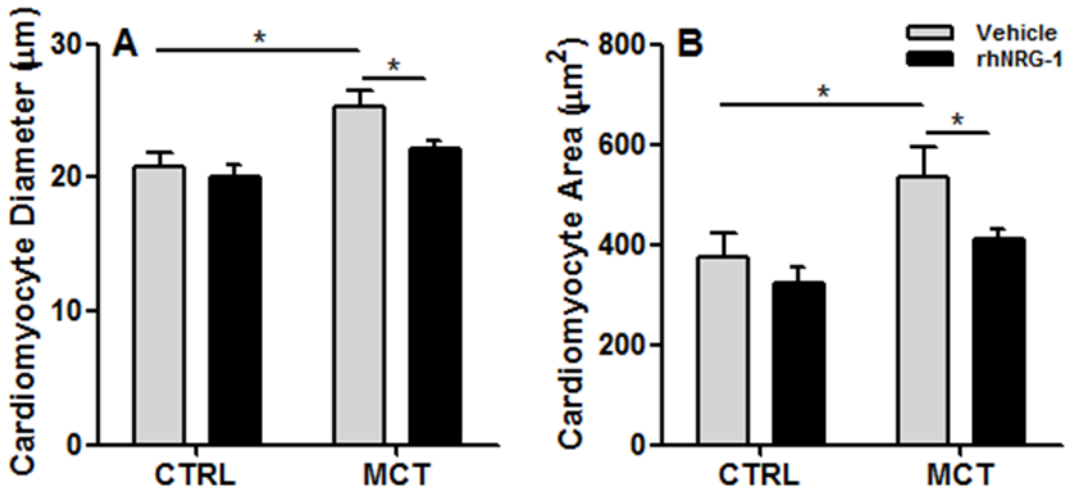

Figure 7 – Quantification of cardiomyocyte dimensions. MCT group animals showed an increased cardiomyocyte diameter (**A**), and cross sectional area (**B**), when compared to control animals. MCT + rhNRG-1 animals showed no differences from the CTRL group, which was also not different from the CTRL + rhNRG-1 group. * $p < 0.05$ in line-targeted groups.

Histological analysis of pulmonary arteries revealed pulmonary hypertension associated vascular remodeling, specifically thickening of the tunica media (53.70 ± 1.11 *vs*. 31.37 ± 0.59 mm, MCT *vs*. CTRL) as seen in Figure 9-A. Media area/ lumen area ratio was also increased in MCT animals (41.19 ± 1.00 *vs*. 31.89 ± 1.84 %, MCT *vs*. CTRL, Figure 9-B). Administration of rhNRG-1 resulted in reversal of the detected remodeling (34.26 ± 0.61 mm and 30.33 ± 1.74 %).

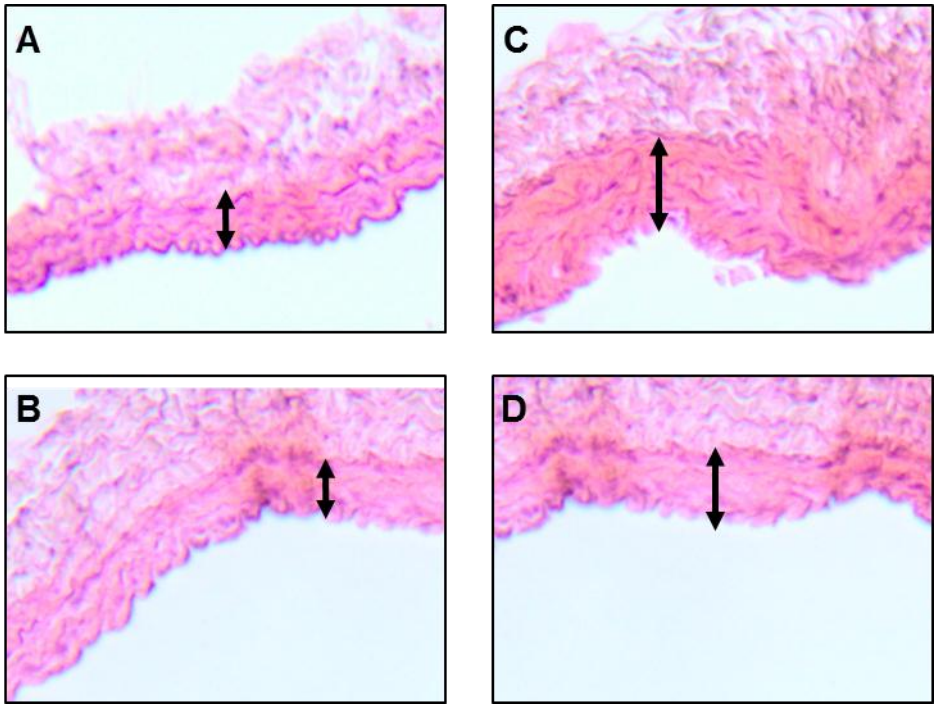

Figure 8 – Histological analysis of pulmonary arterial rings structure. **.** Light microscopy images of hematoxylin-eosin stained sections of pulmonary arterial rings (63x) from CTRL + vehicle (**A**), CTRL + rhNRG-1 (**B**), MCT + vehicle (**C**) and MCT + rhNRG-1 (**D**).

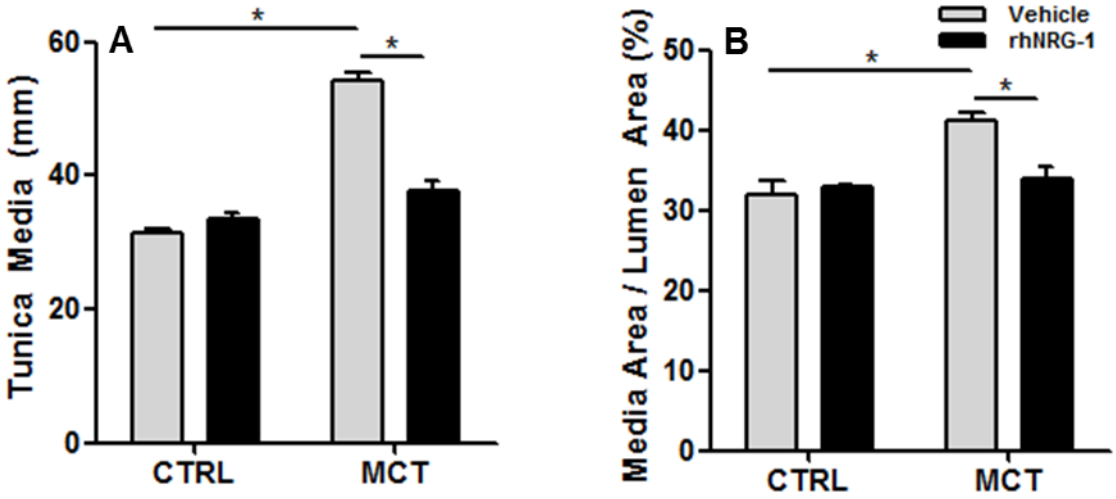

Figure 9 – Quantification of pulmonary arterial rings media thickness. MCT group showed increased thickness of the media layer (**A**) and the media layer area / lumen area ratio (**B**), while the rhNRG-1 group showed non-significant differences from the CTRL group. * $p < 0.05$ in line-targeted groups.

Compared to healthy animals, MCT animals showed increased fibrosis in the RV (2.04 ± 0.17 *vs*. 0.98 ± 0.07 %, MCT *vs*. CTRL), while MCT treated rats showed no differences from the control group (1.00 ± 0.17 %) as represented in Figures 10-11.

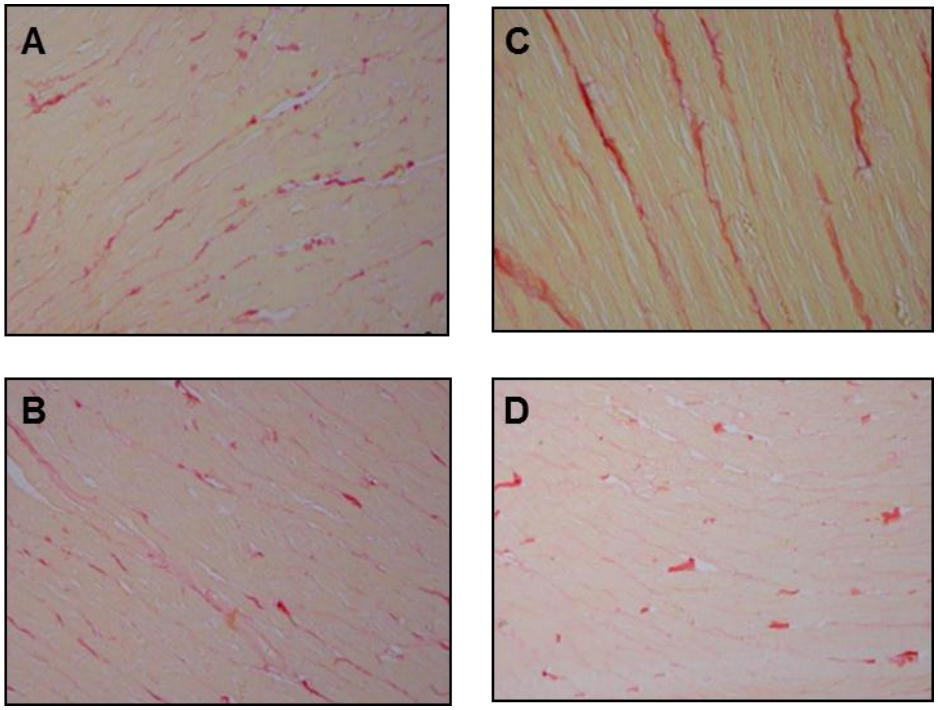

Figure 10 –Histological analysis of RV fibrosis. Light microscopy images of sirius red stained samples of RV (400x) from CTRL + vehicle (A), CTRL + rhNRG-1 (B), MCT + vehicle (C) and MCT + rhNRG-1 (D).

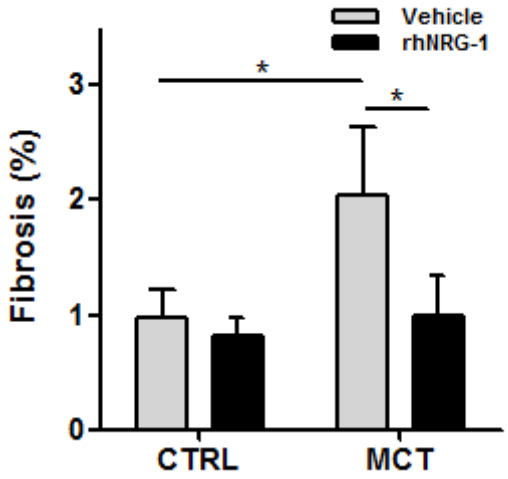

Figure 11 – Quantification of RV fibrosis. MCT group animals showed increased fibrosis when compared to CTRL animals, while MCT + rhNRG-1 are not different from the CTRL group. rhNRG-1 did not increase fibrosis in CTRL animals (**C**). * $p < 0.05$ in line-targeted groups.

Molecular studies

The RV from MCT animals presented increased mRNA expression of brain natriuretic peptide (BNP) and endothelin (ET)-1 (17.46 ± 2.18 *vs*. 1.00 ± 0.42, 5.03 ±

1.24 *vs*. 1.00 ± 0.21 AU, MCT *vs*. CTRL, respectively), as illustrated in Figure 12-A,B. Endogenous levels of NRG-1 expression were also higher in the MCT animals (11.05 ± 2.85 *vs*. 1.00 ± 0.30 AU, MCT *vs*. CTRL). These changes were attenuated or reversed in the MCT + rhNRG-1 group (5.57 ± 1.99, 1.73 ± 0.66, 0.73 ± 0.36, respectively) as represented in Figure 12-C. Treating MCT animals with bosentan resulted in decreased levels of NRG-1 when compared with MCT animals (3.79 ± 1.47 *vs*. 11.05 ± 2.85 AU, MCT_{BOS} *vs*. MCT).

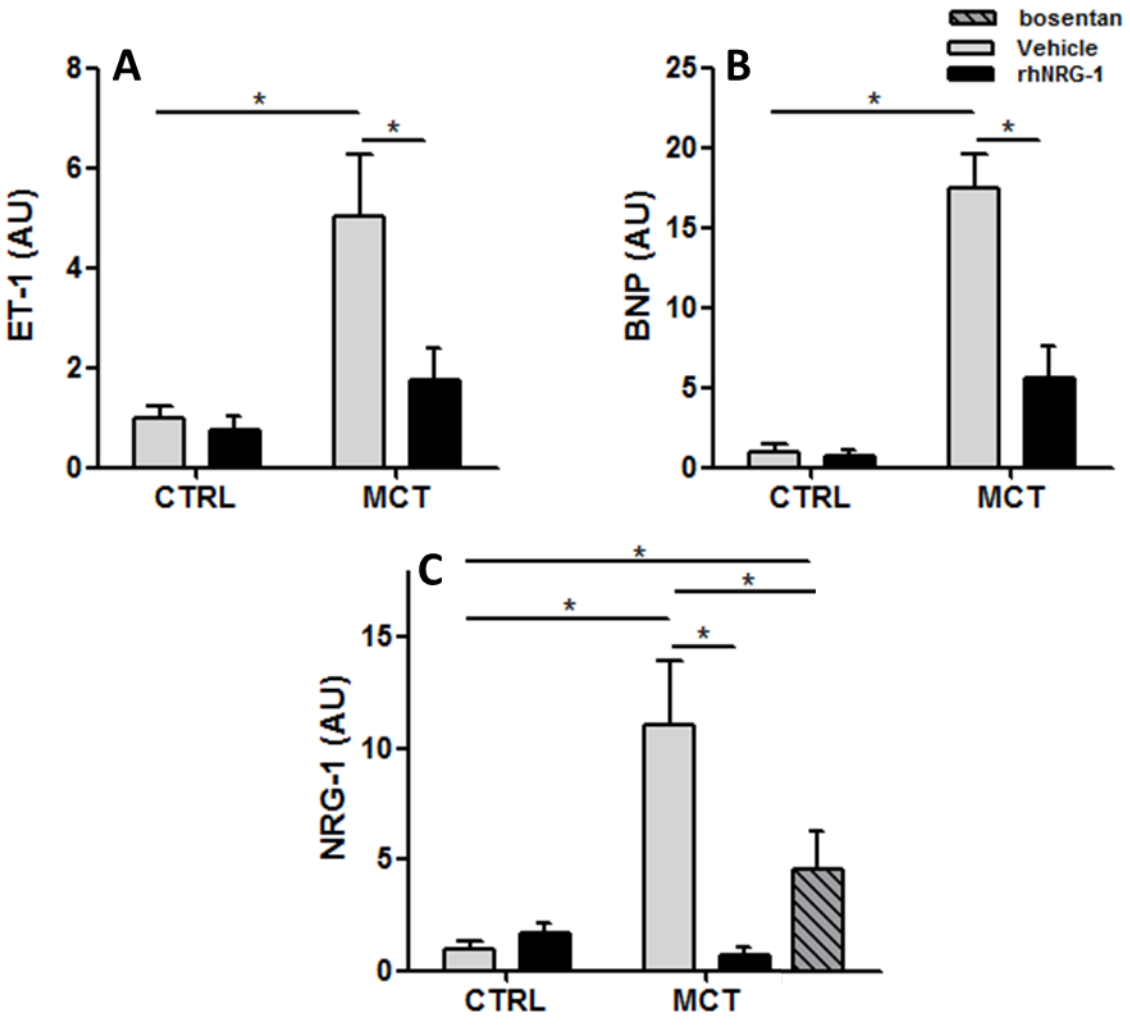

Figure 12 – mRNA quantification of BNP, ET-1 and NRG-1 in the RV. MCT group showed increased expression of ET-1 (**A**), while the rhNRG-1 group showed significantly lower levels of expression. The MCT group also showed increased expression of BNP (**B**) while the rhNRG-1 group showed no significant differences from the CTRL group. NRG-1 levels were increased in the MCT group (**C**) and treatment with rhNRG-1 resulted in no differences from the CTRL animals. Treating MCT animals with bosentan resulted in decreased levels of NRG-1 expression when compared to the MCT group. * $p < 0.05$ in line-targeted groups.

rhNRG-1 treatment improves RV and LV function in MCT-induced pulmonary hypertension

In this work we demonstrated that chronic treatment with intraperitoneal administration of rhNRG-1, in a model of MCT-induced PAH, enhances both LV and RV function, improving CO and attenuating increased overload-dependent systolic and diastolic dysfunction.

Several studies have demonstrated the progression of MCT-induced pulmonary hypertension using several indexes of RV function and structure through echocardiography.

Non-invasive methods to evaluate RV function and severity of PAH are of major importance and allow a comparable approach to that used more routinely in patients.

Transthoracic echocardiography is used to assess temporal evolution of cardiac dysfunction in PAH [173-175], specifically pulmonary waveform and flow. In MCT-induced PAH there's a development of a midsystolic notch in the pulmonary artery flow waveform (which corresponds to the findings we have observed in our study – Figure 1) together with quantifiable reverse flow (pulmonary regurgitation), and decreased acceleration time. Coinciding, we have also observed a decrease in PAAT which significantly altered the PAAT/PAET ratio, and systolic flow which is compromised in PAH and is associated with pulmonary systolic pressures [176] and correlates with decreased survival in PAH patients [177]. Treating rats with rhNRG-1 resulted in the absence of pulmonary midsystolic rapid deceleration, observed by the absence of a misystolic notch in the pulmonary waveform of MCT+NRG-1 animals (Figure 1). Pulmonary flow velocity and acceleration time were also restored with rhNRG-1 pharmacological intervention, revealing an improved pulmonary arterial function and decreased RV afterload.

Similarly to previous studies [173], we observed a trend towards RV chamber dilation, nevertheless significance was not achieved (data not shown). This might easily be explained by the stage at which the animals were analyzed (21-24 days after MCT administration). At this time point, the RV, in response to increased pulmonary vascular resistances, presents a non-dilated, adaptive concentric hypertrophied chamber. In fact, Hardziyenka et al [178] have shown that right ventricular end-diastolic diameter, measured by echocardiography seems to start to increase between 20-25 days post MCT administration. This study showed that, in response to increased pressure-overload, there is a shift of the intraventricular septum to the left side chamber,

agreeing with our observations (Figure 1). NRG-1 therapeutic intervention attenuated the adaptive hypertrophy, improving RV structure, as well as correcting intraventricular septum ablation.

In PAH, not only RV function is impaired, LV function might also be impaired due to ventricular interaction and decreased right sided function [19]. Therefore it is crucial to evaluate the LV in the context of PAH [179], whose diastolic impairment is closely related to PAH severity, as evaluated by echo-doppler [180]. We observed a significant decrease in LVEDD as well as decreased aortic flow velocity, corroborating the effect that unloading of the LV through RV alterations in PAH has on the left side function [31].

Although no studies have invasively evaluated NRG-1's chronic treatment effect on RV function in PAH, enough studies have been performed on the LV that allow us to explain our results. Cardiac performance was improved by NRG-1 administration in several models of cardiovascular disorders. Liu et al [147], used models of myocardial ischemia, anthracycline-induced cardiomyopathy, and chronic pacing, and showed that NRG-1 treatment leads to attenuation of contractile dysfunction. LVEF and LVESP were decreased, as well as dP/dt_{max} with animals with heart failure, while treated animals showed improvements in all parameters. Diastolic function was also preserved with treatment as measured by LVEDP and dP/dt_{min} [147]. In diabetic cardiomyopathy animal models, NRG-1 treatment also resulted in improvement of both systolic and diastolic function [151]. Similarly, and despite all the structural differences between the LV and the RV, our results in the RV function match what has been previously described for the LV. MCT-injected animals revealed a severe cardiac dysfunction secondary to PAH. MCT animals presented RV hypercontractility, as shown by highly increased systolic pressures, as well by changes in other parameters of contractile function, namely dP/dt_{max} and inferior vena cava occlusion-derived ESPV relationship's slope. Diastolic dysfunction was also present in the RV of MCT animals, shown by increased stiffness (rise in RVEDP) and impaired relaxation (decreased RV – dP/dt_{min}). These hemodynamic alterations correspond to an initial compensatory myocardial hypertrophy of the RV in response to pressure overload resulting from increased pulmonary vascular resistance, as described in previous works [181].

As earlier mentioned, LV dysfunction is associated with PAH and RV pressure overload [30,31]. Our echocardiographic analysis revealed altered LV structure in PAH induced animals which might result in altered diastolic and systolic function. Moreover, ventricular interaction is responsible for RV-dependent alterations of the LV [32], and

both animal [182] and human [30] data have demonstrated that systolic function is impaired in RV pressure overload.

Our data have also showed that not only the RV was affected, but also the left side of the heart presented both systolic and diastolic dysfunction secondary to the pressure-overloaded RV. Contractile capacity was compromised as well as cardiac output, and diastolic function impaired with decreased d/dt_{min}, increased τ and increased EDPVR-derived slope (k1).

Treating MCT animals with NRG-1 resulted in the improvement of RV and LV function. Both systolic and diastolic dysfunction of the RV and the LV were improved and both ventricles showed enhanced contractile and relaxation functions.

Cardiac catheterization allowed for a more detailed analysis of ventricular function, and corroborated echocardiographic data, nevertheless one has to be careful when interpreting the results and extrapolating previous knowledge from the LV and using them to explain RV pathophysiology [19].

Stem cell treatment improves RV function in the MCT-induced model of PAH [183,184], as well as in a biventricular failure model [185]. Taking into account that NRG-1 plays a key role in the differentiation of cardiomyocytes [113,114], this could be a very interesting new approach in the understanding and development of NRG-1 associated treatment of PAH. In fact, further comprehension of these effects in human patients is not that far away since RV-associated disorders are already producible at a cell culture level [186], creating new research possibilities.

Myocardial hypertrophy is accompanied by a significant increase in the content of extracellular matrix proteins, therefore a change in tension development seen in multicellular preparations may be due merely to a change in the number of force-generating elements per cross-sectional area of myocardium, without an actual change in intrinsic contractile protein function. Thus, it was important to complement our hemodynamic data with the information gathered from skinned cardiomyocytes in the absence of confounding influences of extracellular matrix components.

Pressure-overload on the RV results in increased sarcomeric stiffness [187]. Our evaluation of single cell contractile machinery showed increased stiffness in MCT-induced PAH, as cardiomyocytes from the MCT group revealed increased passive force development at several sarcomeric lengths, confirming at the cellular level, what had been previously described in our *in vivo* analysis, and suggesting that the increased stiffness and impaired relaxation of the RV in PAH is in part due to increased sarcomere stiffness. Active force enhancement further corroborates the RV hypercontractile state in response to pressure-overload observed in our model.

Protein kinase C-alpha phosphorylation of titin leads to increased passive tension [188], and on the onset of PAH, in animal models, its expression levels are increased [189,190]. In the MCT-induced PAH model, increased oxidative stress, through reactive oxygen species production is associated with RV failure [191], and also increases titin stiffness through disulfide bonding in a N2B specific sequence [192], which might explain the observed increased passive tension in cardiomycoytes isolated from theMCT groupBoth phosphorylation of titin domains, and titin isoform shifting to the less compliant isoform (N2B) are associated with neurohumoral activation [193], that is present in MCT-induced PAH [163].

Our pharmacological intervention resulted in improved intrinsic myocardial performance, attenuation of the increased stiffness observed in MCT cardiomyocytes, as well as of the overdevelopment of active force. Attenuated stiffness in the MCT + rhNRG-1 group could be explained by the cardioprotective effects of NRG-1 through oxidative stress reduction [194,195].

Taking all the functional evaluations into account, we can clearly state that rhNRG-1 significantly improves RV function both at the intrinsic myocardial function level, ventriculo-arterial coupling, with improved blood pumping capability and improved pulmonary flow patterns.

Interestingly CTRL + rhNRG-1 skinned cardiomyocytes revealed decreased passive tension when compared to the CTRL + vehicle group, demonstrating an effect of NRG-1 in non-pathological conditions over sarcomeric determinants. A possible mechanism through which passive tension decreases in control treated animals is the protein kinase G-dependent phosphorylation of a serine residue within the N2B fragment of titin [196], through NRG-1 mediated activation of PI3K/Akt and eNOS [124,197], leading to a decreased stiffness of the cardiomyocyte myofibrils.

Therefore, NRG-1 may ameliorate RV compliance and diastolic function by affecting the sarcomeric protein titin and by activation of the eNOS, both powerful determinants of ventricular compliance.

PAH-associated pulmonary vascular dysfunction and remodeling is attenuated with rhNRG-1 treatment

PAH is associated with an imbalance of endothelial production of various mediators, resulting in endothelial dysfunction [42]. In the MCT model of PAH, a severe endothelial dysfunction is observed [168,198,199], since once metabolized in the liver, the originated active metabolite (monocrotaline pyrrole) destroys the endothelial layer of pulmonary arteries, and induces vascular remodeling, typical of pulmonary

hypertension [73,77,200], in a similar way to human pathology [201] This is characterized by an impairment in vasorelaxation in response to the well-known endothelium-dependent vasodilator acetylcholine [202].

In fact, in our study pulmonary arteries from MCT-injected animals presented endothelial dysfunction, as they were unable to relax in response to acetylcholine, presenting an increased EC50. These changes might be explained by either an unavailability of acetylcholine receptors or a functional inhibitory effect, through an opposite constrictive response or negative modulation of vasodilatory signaling. Interestingly, in pulmonary vascular dysfunction, there's an impaired vasodilatory response through acetylcholine that is mediated by upregulation of the muscaric acetycholine receptor M1 [203]. Upon stimulation M1 receptor leads to vasoconstriction in opposition to the vasodilataroy response associated with the binding of acetylcholine to the M3 receptor [204], which is dependent on cGMP/eNOS activation. Although controversy exists, some studies have shown that eNOS is downregulated in pulmonary arteries and/or lungs from both animals [205-207] and patients [208] with PAH, including MCT-induced PAH [209,210], and its interaction with intracellular regulatory proteins is also compromised [211].

On the other side, phosphodiesterase-1, which is upregulated in PAH [212,213], is activated through inositol triphosphate-mediated intracellular calcium release, in response to M1 receptor activation. This enzymatic activation leads to cGMP degradation [214], and might lead to depressed levels of cGMP-dependent NO production.

In our study, chronic treatment with rhNRG-1 resulted in improved pulmonary arterial endothelial function, which might be a result of increased eNOS activation [215]. Nevertheless, further studies need to be performed in order to determine which signaling pathways are altered in our animal model of PAH, and if eNOS activation through NRG-1/ErbB signaling is the major contributor to the improved endothelial function.

Besides endothelial dysfunction, vascular remodeling was also observed in pulmonary arteries from the MCT-injected animals, through thickening of the smooth muscle cell comprised media layer.

The media area/lumen area ratio gives us a more detailed analysis of the structural changes happening at the pulmonary arteries. Maximum vasodilation should be achieved prior to histological analysis of the arteries, in order to exclude bias in lumen area in vasoconstricted arteries [216].

Despite significant increase in medial thickness, no differences in lumen area were observed (data not shown), revealing that remodeling of the pulmonary arterial wall, and not decrease in lumen are taking place in our model of MCT-induced PAH. This finding suggests that the major role in the increase of PVR is a functional decrease of the arterial diameter (vasoconstriction) instead of a structural one (lumen area decrease).

In fact, in our study both measurements reveal increased muscularization of the media layer in MCT-induced PAH animals and, rhNRG-1 treatment resulted in the attenuation of pulmonary vascular remodeling. Intervention with rhNRG-1 completely normalized tunica media thickness, as no significant remodeling was observed in treated animals, diminishing the pulmonary vasculature-imposed overload on the RV.

These results do not differ from other studies that have shown the effect of pharmacological treatment in pulmonary hypertension models, through pulmonary artery remodeling and improved endothelial dysfunction [217-219], and might not come as a surprise, since rhNRG-1 treatment leads to decreased neointima formation and vascular smooth cell proliferation after vascular injury in other vascular beds [131].

MCT-induced RV morphohistological changes are attenuated by rhNRG-1 treatment

rhNRG-1 treatment after PAH-induction resulted in accentuated decrease of cardiac hypertrophy, specifically RV hypertrophy, as well as lung congestion (Table 3). Heart weight was increased in PAH animals, as previously mentioned, and this was analyzed using the HW/BW ratio. Nevertheless, in PAH, the RV is the primary affected ventricle and therefore should be the focus of the analysis, since due to the augmented pulmonary vascular resistances it is under pressure overload. And in fact, the RVW/BW ratio was also increased in PAH animals, which revealed the presence of RV hypertrophy.

Despite being in agreement with all of our data regarding hypertrophy and hypertrophy-associated parameters measured, the model we're using is associated with cachexia [17,21], and because of that, we alternatively measured the RV/TL ratio which is accepted as a reliable parameter for hypertrophy measurement [22]. The RVW/LV+SW ratio was consistent with the previously mentioned measurements. Lung edema and congestion is a consequence of PAH [220] and using the LW/TL ratio we observed an increase ratio in the MCT group, suggestive of PAH-associated lung fluid retention.

At the cellular level, our model of PAH developed cardiomyocyte hypertrophy, as measured by cardiomyocyte diameter and cross sectional area. These effects were however reverted by rhNRG-1administration. Reversal of hypertrophy in response to treatment underlines the functional recovery observed with non-invasive and invasive hemodynamic measurements. The RV of treated animals is under attenuated pressure-overload and therefore, its adaptative hypertrophic response is decreased. Less muscle mass, less developed force and consequently, attenuated developed pressures and hypercontractile state. Decreased hypertrophy means decreased ventricular stiffness and improved diastolic function, both at the ventricle and the cardiomyocyte level.

Although there is some controversy concerning the presence of interstitial fibrosis in the RV of MCT-injected animals [166,221,222] we have observed increased fibrosis in MCT animals, while treatment with rhNRG-1 resulted in reversal of fibrotic tissue deposition. Fibrotic tissue deposition in PAH aids the development of RV stiffness and contributes to its impaired diastolic function [163], therefore decreasing fibrosis is a major contribution of rhNRG-1 effect in preventing impaired RV relaxation.

Increased expression of cardiac overload and hypertrophy markers are attenuated with rhNRG-1 treatment

Cardiac overload and hypertrophy biomarkers were significantly increased in ill animals, when compared to controls. ET-1 plasmatic levels are elevated in PAH, associated with disease severity [223]. Moreover, its clearance from pulmonary arteries is reduced [224]. ET-1 levels are associated with the development of RV hypertrophy in MCT-induced PAH [82,225] and is increased in this experimental model [163,226]. In our study, RV ET-1 levels were augmented in pulmonary hypertensive rats up to 5-fold. Treatment with rhNRG-1 resulted in the reversal of ET-1 levels to control levels, completely abolishing its MCT-associated increase.

Plasmatic BNP levels are associated with pulmonary hypertension [227] and its production is stimulated in response to pressure-overload [228] and are associated with the extent of RV dysfunction [229], being increased in MCT-injected animals [163]. In the present study, BNP expression in the RV of MCT animals is increased up to 15-fold, and treatment reduces this enhancement by 10-fold.

During the development of several cardiac pathologies in experimental models, NRG-1 cardiac expression rise, in an early stage [102,135,142,144], and in a later phase, when HF is established, its expression drop [102,153]. Moreover, deleting/inhibiting NRG-1 and/or its signaling axis leads to increased susceptibility to

several cardiac-targeted experimental models [102,132,133,138,139]. Human plasmatic quantification has also shown that NRG-1 levels increase and correlate with HF functional class [156]. Although no studies have analyzed NRG-1 levels in the depressed RV, we have shown the increase of NRG-1 mRNA in the RV of rats with PAH induced by MCT, which accordingly to previously mentioned data [102,135,142,144] we interpret as a compensatory response to mechanical strain [215] and hypertrophy [230] induced by the increased pulmonary vascular resistances. Indeed, quantifying NRG-1 RV expression of 6 week post MCT-injection animals (data not shown) revealed lower mRNA expression than 4 week post MCT animals, which correlate with the decompensated, RV failure phase of PAH, where increased angiotensin II and epinephrine levels, associated with HF negatively regulate NRG-1 expression [215].

Indeed, neurohumoral activation is associated with RV dysfunction in PAH [231]. While there is a downregulation of beta-adrenergic receptors [232] in late-stage MCT-induced PAH, both epinephrine and norepinephrine levels are increased [232,233]. The renin-angiotensin-aldosterone system is dysregulated in PAH [234], and contributes to pulmonary vascular remodeling [235]. Increased expression of the angiotensin-converting enzyme in pulmonary arteries of PAH patients [236] and increased activity in failing RVs [237], might account for the increased levels of angiotensin II. Dysregulation of neurohumoral mediators with increase of both epinephrine and angiotensin II results in an inhibiting effect on NRG-1 synthesis [215], explaining its downregulation in later stages of PAH with RV failure (6 week MCT animals).

NRG-1 expression is induced in response to ET-1 action on endothelial cells [215,230], and this tight association was observed in our experimental groups, where higher expression levels of ET-1 and endogenous NRG-1 were observed in the MCT-group, while treatment with NRG-1 led to a normalization of these levels. Also, treating MCT animals with bosentan, a non-selective ET-1 receptor antagonist led to decreased NRG-1 levels, confirming the connection between ET-1 stimulation and NRG-1 increased synthesis. Nevertheless, the relation between ET-1 and NRG-1 is not clearly understood. While ET-1 increased coincided with NRG-1 increase, treatment with exogenous NRG-1 resulted in decreased ET-1 expression. While no explained mechanism justifies this result, an association between ET_A (ET-1 receptor) and ErbB2/4 has been described [164], where colocalization of ET_A and ErbB2/4 is determined to be the T-tubules in adult cardiomyocytes. This proximal physical localization, favors a physiological interaction, where ET-1-mediated stimulation inhibits

ErbB2/4 activation [164] in a one way manner (i.e. ET_A activation inhibits ErbB2/4, while ErbB2/4 activation does not inhibit ET_A). This inhibitory relationship confirms the relation between ET-1/NRG-1, and opens a possible detrimental mechanism for ET-1 overexpression in PAH. Despite this, ET-1's decreased levels in NRG-1 treatment are not answered for. One could hypothesize that being administered exogenously and at high dosages, NRG-1 can overcome the ET-1-mediated inhibitory effects and not only activate ErbB2/4, but exert some kind of negative regulation on ET-1/ET_A signaling.

On the other hand, simply by improving vascular function, as observed by the improved endothelial function of pulmonary arteries in MCT-induced PAH animals treated with NRG-1, and therefore reducing pulmonary vascular resistances, RV pressure overload was significantly attenuated. This means that decreased mechanical strain on the RV, which as mentioned above, has a stimulatory effect on NRG-1 production and positively regulates ET-1 synthesis in endothelial cells [238]. Therefore, decreasing mechanical strain by NRG-1 treatment might be the link between ET-1 and NRG-1 decreased levels following treatment, nevertheless this association needs to be further studied.

CONCLUSION

In conclusion, we show for the first time, in an experimental model of MCT-induced PAH, that rhNRG-1 treatment is able to restore PAH-induced severe abnormalities in cardiopulmonary function and structure.

PAH is a chronic disease that is not always diagnosed early, therefore an increased interest is achieved in our approach where we begin treatment after PAH is established, revealing a more practical and clinical relevant therapy.

The NRG-1/ErbB4 system has been thoroughly studied in the cardiovascular system, but research so far has failed to determine its effects on normal or diseased RV physiology, or pulmonary vascular function. We have set out and demonstrated the effects of an increase in NRG-1 levels through exogenous administration of the protein, which has shown that specific activation of ErbB receptors mediates several compensatory mechanisms that ameliorate the dysfunction and structural abnormalities associated with PAH.

In spite of these results, further research is needed in order to determine specifically where NRG-1 plays its major role. Both ventricular and pulmonary function are altered, but since in this model RV dysfunction and eventual failure is secondary to pah, we cannot ascertain whether RV function and structure improvement is secondary to pulmonary vascular functional enhancement and therefore decreased vascular resistances, or if NRG-1 has a direct effect on the ventricle which by itself is capable of leading to the changes we observed.

Although this question remains unanswered, the importance of this system in the RV, and more importantly in the pathophysiology of PAH is undeniable and therefore constitutes a major research interest.

Also it is important to take into account that the animal model used in the present study does not mimic in its entirety human PH or PAH, nevertheless it has several pathophysiological alterations in common that allow us to enthusiastically point NRG-1 as a possible novel treatment for a very devastating, uncured and with an uncertain prognosis disease.

We hope to have opened the road for further basic and translational research that could possibly lead to the establishment of rhNRG-1 as a novel and safe therapeutic agent for treating patients with PAH and RVHF.

BIBLIOGRAPHY

1 Romberg, E. (1981) Über Sklerose der Lungen Arterie. *Dtsch Arch Klin Med* 48, 197-206

2 Fishman, A.P. (2004) A century of pulmonary hemodynamics. *Am J Respir Crit Care Med* 170 (2), 109-113

3 Brenner, O. (1935) Pathology of the vessels of the pulmonary circulation. *Arch Intern Med J* 56, 211–237, 457–497, 724–752, 976–1014, 1190–1241

4 Dresdale, D.T. et al. (1954) Recent studies in primary pulmonary hypertension, including pharmacodynamic observations on pulmonary vascular resistance. *Bull N Y Acad Med* 30 (3), 195-207

5 Clauss, R.H. et al. (1956) Influence of acetylcholine on human pulmonary circulation under normal and hypoxic conditions. *Proc Soc Exp Biol Med* 93 (1), 77-79

6 Gurtner, H.P. (1985) Aminorex and pulmonary hypertension. A review. *Cor Vasa* 27 (2-3), 160-171

7 Lourenco, A.P. et al. (2012) Current pathophysiological concepts and management of pulmonary hypertension. *Int J Cardiol* 155 (3), 350-361

8 Galie, N. et al. (2004) Guidelines on diagnosis and treatment of pulmonary arterial hypertension. The Task Force on Diagnosis and Treatment of Pulmonary Arterial Hypertension of the European Society of Cardiology. *Eur Heart J* 25 (24), 2243-2278

9 Humbert, M. et al. (2006) Pulmonary arterial hypertension in France: results from a national registry. *Am J Respir Crit Care Med* 173 (9), 1023-1030

10 Peacock, A.J. et al. (2007) An epidemiological study of pulmonary arterial hypertension. *Eur Respir J* 30 (1), 104-109

11 Ghio, S. et al. (2001) Independent and additive prognostic value of right ventricular systolic function and pulmonary artery pressure in patients with chronic heart failure. *J Am Coll Cardiol* 37 (1), 183-188

12 Leite-Moreira, A.F. (2006) Current perspectives in diastolic dysfunction and diastolic heart failure. *Heart* 92 (5), 712-718

13 Murray, C.J. and Lopez, A.D. (1997) Alternative projections of mortality and disability by cause 1990-2020: Global Burden of Disease Study. *Lancet* 349 (9064), 1498-1504

14 McLaughlin, V.V. et al. (2009) ACCF/AHA 2009 expert consensus document on pulmonary hypertension a report of the American College of Cardiology Foundation Task Force on Expert Consensus Documents and the American Heart Association developed in collaboration with the American College of Chest Physicians; American Thoracic Society, Inc.; and the Pulmonary Hypertension Association. *J Am Coll Cardiol* 53 (17), 1573-1619

15 Yang, X. et al. (2005) Dysfunctional Smad signaling contributes to abnormal smooth muscle cell proliferation in familial pulmonary arterial hypertension. *Circ Res* 96 (10), 1053-1063

16 Morrell, N.W. et al. (2001) Altered growth responses of pulmonary artery smooth muscle cells from patients with primary pulmonary hypertension to transforming growth factor-beta(1) and bone morphogenetic proteins. *Circulation* 104 (7), 790-795

17 Newman, J.H. et al. (2004) Genetic basis of pulmonary arterial hypertension: current understanding and future directions. *J Am Coll Cardiol* 43 (12 Suppl S), 33S-39S

18 MacLean, M.R. and Dempsie, Y. (2009) Serotonin and pulmonary hypertension--from bench to bedside? *Curr Opin Pharmacol* 9 (3), 281-286

19 Voelkel, N.F. et al. (2006) Right ventricular function and failure: report of a National Heart, Lung, and Blood Institute working group on cellular and molecular mechanisms of right heart failure. *Circulation* 114 (17), 1883-1891

20 van Wolferen, S.A. et al. (2007) Prognostic value of right ventricular mass, volume, and function in idiopathic pulmonary arterial hypertension. *Eur Heart J* 28 (10), 1250-1257

21 Ghio, S. et al. (2010) Prognostic relevance of the echocardiographic assessment of right ventricular function in patients with idiopathic pulmonary arterial hypertension. *Int J Cardiol* 140 (3), 272-278

22 D'Alonzo, G.E. et al. (1991) Survival in patients with primary pulmonary hypertension. Results from a national prospective registry. *Ann Intern Med* 115 (5), 343-349

23 Sandoval, J. et al. (1994) Survival in primary pulmonary hypertension. Validation of a prognostic equation. *Circulation* 89 (4), 1733-1744

24 Maxwell, A.J. and Bridges, N.D. (2001) Pediatric Primary Pulmonary Hypertension. *Curr Treat Options Cardiovasc Med* 3 (5), 371-383

25 Ritchie, M. et al. (1993) Echocardiographic characterization of the improvement in right ventricular function in patients with severe pulmonary hypertension after single-lung transplantation. *J Am Coll Cardiol* 22 (4), 1170-1174

26 Reesink, H.J. et al. (2007) Reverse right ventricular remodeling after pulmonary endarterectomy in patients with chronic thromboembolic pulmonary hypertension: utility of magnetic resonance imaging to demonstrate restoration of the right ventricle. *J Thorac Cardiovasc Surg* 133 (1), 58-64

27 Bogaard, H.J. et al. (2009) The right ventricle under pressure: cellular and molecular mechanisms of right-heart failure in pulmonary hypertension. *Chest* 135 (3), 794-804

28 Bogaard, H.J. et al. (2009) Chronic pulmonary artery pressure elevation is insufficient to explain right heart failure. *Circulation* 120 (20), 1951-1960

29 Chang, S.M. et al. (2007) Pulmonary hypertension and left heart function: insights from tissue Doppler imaging and myocardial performance index. *Echocardiography* 24 (4), 366-373

30 Dong, S.J. et al. (1995) Regional left ventricular systolic function in relation to the cavity geometry in patients with chronic right ventricular pressure overload. A three-dimensional tagged magnetic resonance imaging study. *Circulation* 91 (9), 2359-2370

31 Menzel, T. et al. (2000) Pathophysiology of impaired right and left ventricular function in chronic embolic pulmonary hypertension: changes after pulmonary thromboendarterectomy. *Chest* 118 (4), 897-903

32 Slinker, B.K. and Glantz, S.A. (1986) End-systolic and end-diastolic ventricular interaction. *Am J Physiol* 251 (5 Pt 2), H1062-1075

33 Weir, E.K. et al. (1989) The acute administration of vasodilators in primary pulmonary hypertension. Experience from the National Institutes of Health Registry on Primary Pulmonary Hypertension. *Am Rev Respir Dis* 140 (6), 1623-1630

34 Rich, S. and Brundage, B.H. (1987) High-dose calcium channel-blocking therapy for primary pulmonary hypertension: evidence for long-term reduction in pulmonary arterial pressure and regression of right ventricular hypertrophy. *Circulation* 76 (1), 135-141

35 Nef, H.M. et al. (2010) Pulmonary hypertension: updated classification and management of pulmonary hypertension. *Heart* 96 (7), 552-559

36 Sitbon, O. et al. (2005) Long-term response to calcium channel blockers in idiopathic pulmonary arterial hypertension. *Circulation* 111 (23), 3105-3111

37 Vane, J.R. et al. (1990) Regulatory functions of the vascular endothelium. *N Engl J Med* 323 (1), 27-36

38 Geraci, M.W. et al. (1999) Pulmonary prostacyclin synthase overexpression in transgenic mice protects against development of hypoxic pulmonary hypertension. *J Clin Invest* 103 (11), 1509-1515
39 Hoshikawa, Y. et al. (2001) Prostacyclin receptor-dependent modulation of pulmonary vascular remodeling. *Am J Respir Crit Care Med* 164 (2), 314-318
40 Tuder, R.M. et al. (1999) Prostacyclin synthase expression is decreased in lungs from patients with severe pulmonary hypertension. *Am J Respir Crit Care Med* 159 (6), 1925-1932
41 Christman, B.W. et al. (1992) An imbalance between the excretion of thromboxane and prostacyclin metabolites in pulmonary hypertension. *N Engl J Med* 327 (2), 70-75
42 Budhiraja, R. et al. (2004) Endothelial dysfunction in pulmonary hypertension. *Circulation* 109 (2), 159-165
43 Barst, R.J. et al. (1994) Survival in primary pulmonary hypertension with long-term continuous intravenous prostacyclin. *Ann Intern Med* 121 (6), 409-415
44 Higenbottam, T. et al. (1984) Long-term treatment of primary pulmonary hypertension with continuous intravenous epoprostenol (prostacyclin). *Lancet* 1 (8385), 1046-1047
45 Rubin, L.J. et al. (1990) Treatment of primary pulmonary hypertension with continuous intravenous prostacyclin (epoprostenol). Results of a randomized trial. *Ann Intern Med* 112 (7), 485-491
46 Barst, R.J. et al. (1996) A comparison of continuous intravenous epoprostenol (prostacyclin) with conventional therapy for primary pulmonary hypertension. *N Engl J Med* 334 (5), 296-301
47 Olschewski, H. et al. (2002) Inhaled iloprost for severe pulmonary hypertension. *N Engl J Med* 347 (5), 322-329
48 Leuchte, H.H. et al. (2003) Treatment of severe pulmonary hypertension with inhaled iloprost. *Ann Intern Med* 139 (4), 306
49 McLaughlin, V.V. et al. (2010) Addition of inhaled treprostinil to oral therapy for pulmonary arterial hypertension: a randomized controlled clinical trial. *J Am Coll Cardiol* 55 (18), 1915-1922
50 Channick, R.N. et al. (2001) Effects of the dual endothelin-receptor antagonist bosentan in patients with pulmonary hypertension: a randomised placebo-controlled study. *Lancet* 358 (9288), 1119-1123
51 Sitbon, O. et al. (2003) Effects of the dual endothelin receptor antagonist bosentan in patients with pulmonary arterial hypertension: a 1-year follow-up study. *Chest* 124 (1), 247-254
52 Rubin, L.J. et al. (2002) Bosentan therapy for pulmonary arterial hypertension. *N Engl J Med* 346 (12), 896-903
53 Galie, N. et al. (2008) Treatment of patients with mildly symptomatic pulmonary arterial hypertension with bosentan (EARLY study): a double-blind, randomised controlled trial. *Lancet* 371 (9630), 2093-2100
54 Galie, N. et al. (2003) Effects of the oral endothelin-receptor antagonist bosentan on echocardiographic and doppler measures in patients with pulmonary arterial hypertension. *J Am Coll Cardiol* 41 (8), 1380-1386
55 Oudiz, R.J. et al. (2009) Long-term ambrisentan therapy for the treatment of pulmonary arterial hypertension. *J Am Coll Cardiol* 54 (21), 1971-1981
56 Barst, R.J. et al. (2002) Clinical efficacy of sitaxsentan, an endothelin-A receptor antagonist, in patients with pulmonary arterial hypertension: open-label pilot study. *Chest* 121 (6), 1860-1868
57 Galie, N. et al. (2011) Corrigendum to: 'Guidelines for the diagnosis and treatment of pulmonary hypertension' [European Heart Journal (2009) 30, 2493–2537]. The Task Force for the Diagnosis and Treatment of Pulmonary Hypertension of the European Society of Cardiology (ESC) and the European

Respiratory Society (ERS), endorsed by the International Society of Heart and Lung Transplantation (ISHLT). *Eur Heart J* 32 (8), 926

58 Wang, L. et al. (2004) Acute cardiopulmonary effects of a dual-endothelin receptor antagonist on oleic acid-induced pulmonary arterial hypertension in dogs. *Exp Lung Res* 30 (1), 31-42

59 Geiger, R. et al. (2006) Tezosentan decreases pulmonary artery pressure and improves survival rate in an animal model of meconium aspiration. *Pediatr Res* 59 (1), 147-150

60 Persson, B.P. et al. (2009) Inhaled tezosentan reduces pulmonary hypertension in endotoxin-induced lung injury. *Shock* 32 (4), 427-434

61 Lourenco, A.P. et al. (2012) Haemodynamic and neuroendocrine effects of tezosentan in chronic experimental pulmonary hypertension. *Intensive Care Med* 38 (6), 1050-1060

62 Kovalchin, J.P. et al. (1997) Nitric oxide for the evaluation and treatment of pulmonary hypertension in congenital heart disease. *Tex Heart Inst J* 24 (4), 308-316

63 Germann, P. et al. (2005) Inhaled nitric oxide therapy in adults: European expert recommendations. *Intensive Care Med* 31 (8), 1029-1041

64 Galie, N. et al. (2005) Sildenafil citrate therapy for pulmonary arterial hypertension. *N Engl J Med* 353 (20), 2148-2157

65 Machado, R.F. et al. (2005) Sildenafil therapy in patients with sickle cell disease and pulmonary hypertension. *Br J Haematol* 130 (3), 445-453

66 Barnett, C.F. and Machado, R.F. (2006) Sildenafil in the treatment of pulmonary hypertension. *Vasc Health Risk Manag* 2 (4), 411-422

67 Archer, S.L. and Michelakis, E.D. (2009) Phosphodiesterase type 5 inhibitors for pulmonary arterial hypertension. *N Engl J Med* 361 (19), 1864-1871

68 Humbert, M. et al. (2004) Combination of bosentan with epoprostenol in pulmonary arterial hypertension: BREATHE-2. *Eur Respir J* 24 (3), 353-359

69 McLaughlin, V.V. et al. (2006) Randomized study of adding inhaled iloprost to existing bosentan in pulmonary arterial hypertension. *Am J Respir Crit Care Med* 174 (11), 1257-1263

70 Simonneau, G. et al. (2008) Addition of sildenafil to long-term intravenous epoprostenol therapy in patients with pulmonary arterial hypertension: a randomized trial. *Ann Intern Med* 149 (8), 521-530

71 Pabani, S. and Mousa, S.A. (2012) Current and future treatment of pulmonary hypertension. *Drugs Today (Barc)* 48 (2), 133-147

72 Stenmark, K.R. et al. (2009) Animal models of pulmonary arterial hypertension: the hope for etiological discovery and pharmacological cure. *Am J Physiol Lung Cell Mol Physiol* 297 (6), L1013-1032

73 Kay, J.M. et al. (1967) Pulmonary hypertension produced in rats by ingestion of Crotalaria spectabilis seeds. *Thorax* 22 (2), 176-179

74 Okada, M. et al. (1995) Establishment of canine pulmonary hypertension with dehydromonocrotaline. Importance of larger animal model for lung transplantation. *Transplantation* 60 (1), 9-13

75 Gust, R. and Schuster, D.P. (2001) Vascular remodeling in experimentally induced subacute canine pulmonary hypertension. *Exp Lung Res* 27 (1), 1-12

76 Meyrick, B. et al. (1980) Development of Crotalaria pulmonary hypertension: hemodynamic and structural study. *Am J Physiol* 239 (5), H692-702

77 Wilson, D.W. et al. (1989) Progressive inflammatory and structural changes in the pulmonary vasculature of monocrotaline-treated rats. *Microvasc Res* 38 (1), 57-80

78 Stenmark, K.R. et al. (2006) Role of the adventitia in pulmonary vascular remodeling. *Physiology (Bethesda)* 21, 134-145

79 Wagner, J.G. et al. (1993) Characterization of monocrotaline pyrrole-induced DNA cross-linking in pulmonary artery endothelium. *Am J Physiol* 264 (5 Pt 1), L517-522

80 Tanaka, Y. et al. (1996) Site-specific responses to monocrotaline-induced vascular injury: evidence for two distinct mechanisms of remodeling. *Am J Respir Cell Mol Biol* 15 (3), 390-397

81 Shah, M. et al. (2005) Monocrotaline pyrrole-induced endothelial cell megalocytosis involves a Golgi blockade mechanism. *Am J Physiol Cell Physiol* 288 (4), C850-862

82 Miyauchi, T. et al. (1993) Contribution of endogenous endothelin-1 to the progression of cardiopulmonary alterations in rats with monocrotaline-induced pulmonary hypertension. *Circ Res* 73 (5), 887-897

83 Wilson, D.W. et al. (1992) Mechanisms and pathology of monocrotaline pulmonary toxicity. *Crit Rev Toxicol* 22 (5-6), 307-325

84 Itoh, T. et al. (2004) A combination of oral sildenafil and beraprost ameliorates pulmonary hypertension in rats. *Am J Respir Crit Care Med* 169 (1), 34-38

85 Obata, H. et al. (2008) Single injection of a sustained-release prostacyclin analog improves pulmonary hypertension in rats. *Am J Respir Crit Care Med* 177 (2), 195-201

86 Kuwano, K. et al. (2008) A long-acting and highly selective prostacyclin receptor agonist prodrug, 2-{4-[(5,6-diphenylpyrazin-2-yl)(isopropyl)amino]butoxy}-N-(methylsulfonyl)acetam ide (NS-304), ameliorates rat pulmonary hypertension with unique relaxant responses of its active form, {4-[(5,6-diphenylpyrazin-2-yl)(isopropyl)amino]butoxy}acetic acid (MRE-269), on rat pulmonary artery. *J Pharmacol Exp Ther* 326 (3), 691-699

87 Hill, N.S. et al. (1997) Nonspecific endothelin-receptor antagonist blunts monocrotaline-induced pulmonary hypertension in rats. *J Appl Physiol* 83 (4), 1209-1215

88 Prie, S. et al. (1997) The orally active ET(A) receptor antagonist (+)-(S)-2-(4,6-dimethoxy-pyrimidin-2-yloxy)-3-methoxy-3,3-diphe nyl-propionic acid (LU 135252) prevents the development of pulmonary hypertension and endothelial metabolic dysfunction in monocrotaline-treated rats. *J Pharmacol Exp Ther* 282 (3), 1312-1318

89 Yuyama, H. et al. (2004) The orally active nonpeptide selective endothelin ETA receptor antagonist YM598 prevents and reverses the development of pulmonary hypertension in monocrotaline-treated rats. *Eur J Pharmacol* 496 (1-3), 129-139

90 Clozel, M. et al. (2006) Bosentan, sildenafil, and their combination in the monocrotaline model of pulmonary hypertension in rats. *Exp Biol Med (Maywood)* 231 (6), 967-973

91 Cui, B. et al. (2009) CPU0213, a non-selective ETA/ETB receptor antagonist, improves pulmonary arteriolar remodeling of monocrotaline-induced pulmonary hypertension in rats. *Clin Exp Pharmacol Physiol* 36 (2), 169-175

92 Kang, K.K. et al. (2003) DA-8159, a new PDE5 inhibitor, attenuates the development of compensatory right ventricular hypertrophy in a rat model of pulmonary hypertension. *J Int Med Res* 31 (6), 517-528

93 Liu, H. et al. (2007) Oral sildenafil prevents and reverses the development of pulmonary hypertension in monocrotaline-treated rats. *Interact Cardiovasc Thorac Surg* 6 (5), 608-613

94 Izikki, M. et al. (2009) Effects of roflumilast, a phosphodiesterase-4 inhibitor, on hypoxia- and monocrotaline-induced pulmonary hypertension in rats. *J Pharmacol Exp Ther* 330 (1), 54-62

95 Schermuly, R.T. et al. (2004) Chronic sildenafil treatment inhibits monocrotaline-induced pulmonary hypertension in rats. *Am J Respir Crit Care Med* 169 (1), 39-45
96 Yen, C.H. et al. (2010) Sildenafil limits monocrotaline-induced pulmonary hypertension in rats through suppression of pulmonary vascular remodeling. *J Cardiovasc Pharmacol* 55 (6), 574-584
97 Mendes-Ferreira, P. et al. (2012) Therapeutic potential of neuregulin-1 in cardiovascular diseases. *Drug Discovery Today (submitted)*
98 Britsch, S. (2007) The neuregulin-I/ErbB signaling system in development and disease. *Adv Anat Embryol Cell Biol* 190, 1-65
99 Meyer, D. et al. (1997) Isoform-specific expression and function of neuregulin. *Development* 124 (18), 3575-3586
100 Falls, D.L. (2003) Neuregulins: functions, forms, and signaling strategies. *Exp Cell Res* 284 (1), 14-30
101 Luo, X. et al. (2011) Cleavage of neuregulin-1 by BACE1 or ADAM10 protein produces differential effects on myelination. *J Biol Chem* 286 (27), 23967-23974
102 Lemmens, K. et al. (2006) Role of neuregulin-1/ErbB2 signaling in endothelium-cardiomyocyte cross-talk. *J Biol Chem* 281 (28), 19469-19477
103 Yarden, Y. and Sliwkowski, M.X. (2001) Untangling the ErbB signalling network. *Nat Rev Mol Cell Biol* 2 (2), 127-137
104 Meyer, D. and Birchmeier, C. (1995) Multiple essential functions of neuregulin in development. *Nature* 378 (6555), 386-390
105 Cote, G.M. et al. (2005) Neuregulin-1alpha and beta isoform expression in cardiac microvascular endothelial cells and function in cardiac myocytes in vitro. *Exp Cell Res* 311 (1), 135-146
106 Gassmann, M. et al. (1995) Aberrant neural and cardiac development in mice lacking the ErbB4 neuregulin receptor. *Nature* 378 (6555), 390-394
107 Lai, D. et al. (2010) Neuregulin 1 sustains the gene regulatory network in both trabecular and nontrabecular myocardium. *Circ Res* 107 (6), 715-727
108 Lee, K.F. et al. (1995) Requirement for neuregulin receptor erbB2 in neural and cardiac development. *Nature* 378 (6555), 394-398
109 Erickson, S.L. et al. (1997) ErbB3 is required for normal cerebellar and cardiac development: a comparison with ErbB2-and heregulin-deficient mice. *Development* 124 (24), 4999-5011
110 Liu, X. et al. (1998) Domain-specific gene disruption reveals critical regulation of neuregulin signaling by its cytoplasmic tail. *Proc Natl Acad Sci U S A* 95 (22), 13024-13029
111 Camenisch, T.D. et al. (2002) Heart-valve mesenchyme formation is dependent on hyaluronan-augmented activation of ErbB2-ErbB3 receptors. *Nat Med* 8 (8), 850-855
112 Rentschler, S. et al. (2002) Neuregulin-1 promotes formation of the murine cardiac conduction system. *Proc Natl Acad Sci U S A* 99 (16), 10464-10469
113 Zhu, W.Z. et al. (2010) Neuregulin/ErbB Signaling Regulates Cardiac Subtype Specification in Differentiating Human Embryonic Stem Cells. *Circ Res* 107 (6), 776-786
114 Suk Kim, H. et al. (2003) Expression of ErbB receptors in ES cell-derived cardiomyocytes. *Biochem Biophys Res Commun* 309 (1), 241-246
115 Kuramochi, Y. et al. (2004) Cardiac endothelial cells regulate reactive oxygen species-induced cardiomyocyte apoptosis through neuregulin-1beta/erbB4 signaling. *J Biol Chem* 279 (49), 51141-51147
116 Kuramochi, Y. et al. (2004) Myocyte contractile activity modulates norepinephrine cytotoxicity and survival effects of neuregulin-1beta. *Am J Physiol Cell Physiol* 286 (2), C222-229

117 Fukazawa, R. et al. (2003) Neuregulin-1 protects ventricular myocytes from anthracycline-induced apoptosis via erbB4-dependent activation of PI3-kinase/Akt. *J Mol Cell Cardiol* 35 (12), 1473-1479
118 Rohrbach, S. et al. (2005) Apoptosis-modulating interaction of the neuregulin/erbB pathway with anthracyclines in regulating Bcl-xS and Bcl-xL in cardiomyocytes. *J Mol Cell Cardiol* 38 (3), 485-493
119 Bersell, K. et al. (2009) Neuregulin1/ErbB4 signaling induces cardiomyocyte proliferation and repair of heart injury. *Cell* 138 (2), 257-270
120 Baliga, R.R. et al. (1999) NRG-1-induced cardiomyocyte hypertrophy. Role of PI-3-kinase, p70(S6K), and MEK-MAPK-RSK. *Am J Physiol* 277 (5 Pt 2), H2026-2037
121 Lemmens, K. et al. (2004) Neuregulin-1 induces a negative inotropic effect in cardiac muscle: role of nitric oxide synthase. *Circulation* 109 (3), 324-326
122 Zhao, Y.Y. et al. (1999) Neuregulin signaling in the heart. Dynamic targeting of erbB4 to caveolar microdomains in cardiac myocytes. *Circ Res* 84 (12), 1380-1387
123 Okoshi, K. et al. (2004) Neuregulins regulate cardiac parasympathetic activity: muscarinic modulation of beta-adrenergic activity in myocytes from mice with neuregulin-1 gene deletion. *Circulation* 110 (6), 713-717
124 Brero, A. et al. (2010) Neuregulin-1beta1 rapidly modulates nitric oxide synthesis and calcium handling in rat cardiomyocytes. *Cardiovasc Res* 88 (3), 443-452
125 Pentassuglia, L. et al. (2007) Inhibition of ErbB2/neuregulin signaling augments paclitaxel-induced cardiotoxicity in adult ventricular myocytes. *Exp Cell Res* 313 (8), 1588-1601
126 Iivanainen, E. et al. (2007) Intra- and extracellular signaling by endothelial neuregulin-1. *Exp Cell Res* 313 (13), 2896-2909
127 Russell, K.S. et al. (1999) Neuregulin activation of ErbB receptors in vascular endothelium leads to angiogenesis. *Am J Physiol* 277 (6 Pt 2), H2205-2211
128 Yen, L. et al. (2000) Heregulin selectively upregulates vascular endothelial growth factor secretion in cancer cells and stimulates angiogenesis. *Oncogene* 19 (31), 3460-3469
129 Hedhli, N. et al. (2011) Endothelial Derived Neuregulin is an Important Mediator of Ischemic Induced Angiogenesis and Arteriogenesis. *Cardiovasc Res* 111 (10), 1376-1385
130 Panutsopulos, D. et al. (2005) Expression of heregulin in human coronary atherosclerotic lesions. *J Vasc Res* 42 (6), 463-474
131 Clement, C.M. et al. (2007) Neuregulin-1 attenuates neointimal formation following vascular injury and inhibits the proliferation of vascular smooth muscle cells. *J Vasc Res* 44 (4), 303-312
132 Ozcelik, C. et al. (2002) Conditional mutation of the ErbB2 (HER2) receptor in cardiomyocytes leads to dilated cardiomyopathy. *Proc Natl Acad Sci U S A* 99 (13), 8880-8885
133 Crone, S.A. et al. (2002) ErbB2 is essential in the prevention of dilated cardiomyopathy. *Nat Med* 8 (5), 459-465
134 Garcia-Rivello, H. et al. (2005) Dilated cardiomyopathy in Erb-b4-deficient ventricular muscle. *Am J Physiol Heart Circ Physiol* 289 (3), H1153-1160
135 Fang, S.J. et al. (2010) Neuregulin-1 preconditioning protects the heart against ischemia/reperfusion injury through a PI3K/Akt-dependent mechanism. *Chin Med J (Engl)* 123 (24), 3597-3604
136 Hedhli, N. et al. (2011) Endothelium-derived neuregulin protects the heart against ischemic injury. *Circulation* 123 (20), 2254-2262
137 Lemmens, K. et al. (2011) Cardioprotective Effect Of Neuregulin-1 In Myocardial Ischemia-Reperfusion Injury Relies On eNos. *Circulation* 124 (21)

138 Liu, F.F. et al. (2005) Heterozygous knockout of neuregulin-1 gene in mice exacerbates doxorubicin-induced heart failure. *Am J Physiol Heart Circ Physiol* 289 (2), H660-666
139 Vasti, C. et al. (2012) Doxorubicin and NRG-1/erbB4-Deficiency Affect Gene Expression Profile: Involving Protein Homeostasis in Mouse. *ISRN Cardiol* 2012, 1-11
140 Sawyer, D.B. et al. (2002) Modulation of anthracycline-induced myofibrillar disarray in rat ventricular myocytes by neuregulin-1beta and anti-erbB2: potential mechanism for trastuzumab-induced cardiotoxicity. *Circulation* 105 (13), 1551-1554
141 Timolati, F. et al. (2006) Neuregulin-1 beta attenuates doxorubicin-induced alterations of excitation-contraction coupling and reduces oxidative stress in adult rat cardiomyocytes. *J Mol Cell Cardiol* 41 (5), 845-854
142 Doggen, K. et al. (2009) Deficient Cardiac Neuregulin-ErbB Signaling in Type 2 Diabetes, and Beneficial Effects of Treatment With Neuregulin-1. *Circulation* 120 (18), S828-S828
143 Gui, C. et al. (2012) Neuregulin-1/ErbB signaling is impaired in the rat model of diabetic cardiomyopathy. *Cardiovasc Pathol* 21 (5), 414-420
144 Doggen, K. et al. (2009) Ventricular ErbB2/ErbB4 activation and downstream signaling in pacing-induced heart failure. *J Mol Cell Cardiol* 46 (1), 33-38
145 Rohrbach, S. et al. (1999) Neuregulin in cardiac hypertrophy in rats with aortic stenosis. Differential expression of erbB2 and erbB4 receptors. *Circulation* 100 (4), 407-412
146 Guo, Y.F. et al. (2012) Neuregulin-1 attenuates mitochondrial dysfunction in a rat model of heart failure. *Chin Med J (Engl)* 125 (5), 807-814
147 Liu, X. et al. (2006) Neuregulin-1/erbB-activation improves cardiac function and survival in models of ischemic, dilated, and viral cardiomyopathy. *J Am Coll Cardiol* 48 (7), 1438-1447
148 Gu, X. et al. (2010) Cardiac functional improvement in rats with myocardial infarction by up-regulating cardiac myosin light chain kinase with neuregulin. *Cardiovasc Res* 88 (2), 334-343
149 Xiao, J. et al. (2012) Therapeutic effects of neuregulin-1 gene transduction in rats with myocardial infarction. *Coron Artery Dis* 23 (7), 460-468
150 Bian, Y. et al. (2009) Neuregulin-1 attenuated doxorubicin-induced decrease in cardiac troponins. *Am J Physiol Heart Circ Physiol* 297 (6), H1974-1983
151 Li, B. et al. (2011) Therapeutic effects of neuregulin-1 in diabetic cardiomyopathy rats. *Cardiovasc Diabetol* 10, 69
152 Li, J. et al. (2007) [Effects of recombined human neuregulin on the contractibility of cardiac muscles of rhesus monkeys with pacing-induced heart failure]. *Sichuan Da Xue Xue Bao Yi Xue Ban* 38 (1), 105-108
153 Doggen, K. et al. (2008) Myocardial neuregulin-1/ErbB signalling is activated during diabetes. *Acta Cardiol* 63 (1), 113-113
154 Seidman, A. et al. (2002) Cardiac dysfunction in the trastuzumab clinical trials experience. *J Clin Oncol* 20 (5), 1215-1221
155 Rohrbach, S. et al. (2005) Neuregulin receptors erbB2 and erbB4 in failing human myocardium -- depressed expression and attenuated activation. *Basic Res Cardiol* 100 (3), 240-249
156 Ky, B. et al. (2009) Neuregulin-1 beta is associated with disease severity and adverse outcomes in chronic heart failure. *Circulation* 120 (4), 310-317
157 Xu, G. et al. (2009) Preventive effects of heregulin-beta1 on macrophage foam cell formation and atherosclerosis. *Circ Res* 105 (5), 500-510
158 Anna Geisberg, C. et al. (2011) Circulating neuregulin-1beta levels vary according to the angiographic severity of coronary artery disease and ischemia. *Coron Artery Dis* 22 (8), 577-582

159 Perik, P.J. et al. (2007) Serum HER2 levels are increased in patients with chronic heart failure. *Eur J Heart Fail* 9 (2), 173-177
160 Posch, M.G. et al. (2010) Plasma HER2 levels are not associated with cardiac function or hypertrophy in control subjects and heart failure patients. *Int J Cardiol* 145 (1), 105-106
161 Gao, R. et al. (2010) A Phase II, randomized, double-blind, multicenter, based on standard therapy, placebo-controlled study of the efficacy and safety of recombinant human neuregulin-1 in patients with chronic heart failure. *J Am Coll Cardiol* 55 (18), 1907-1914
162 Jabbour, A. et al. (2011) Parenteral administration of recombinant human neuregulin-1 to patients with stable chronic heart failure produces favourable acute and chronic haemodynamic responses. *Eur J Heart Fail* 13 (1), 83-92
163 Lourenco, A.P. et al. (2006) Myocardial dysfunction and neurohumoral activation without remodeling in left ventricle of monocrotaline-induced pulmonary hypertensive rats. *Am J Physiol Heart Circ Physiol* 291 (4), H1587-1594
164 Chung, K.Y. and Walker, J.W. (2007) Interaction and inhibitory cross-talk between endothelin and ErbB receptors in the adult heart. *Mol Pharmacol* 71 (6), 1494-1502
165 Schafer, S. et al. (2009) Chronic inhibition of phosphodiesterase 5 does not prevent pressure-overload-induced right-ventricular remodelling. *Cardiovasc Res* 82 (1), 30-39
166 Lourenco, A.P. et al. (2011) A Western-type diet attenuates pulmonary hypertension with heart failure and cardiac cachexia in rats. *J Nutr* 141 (11), 1954-1960
167 Falcao-Pires, I. et al. (2011) Diabetes mellitus worsens diastolic left ventricular dysfunction in aortic stenosis through altered myocardial structure and cardiomyocyte stiffness. *Circulation* 124 (10), 1151-1159
168 Mam, V. et al. (2010) Impaired vasoconstriction and nitric oxide-mediated relaxation in pulmonary arteries of hypoxia- and monocrotaline-induced pulmonary hypertensive rats. *J Pharmacol Exp Ther* 332 (2), 455-462
169 Falcao-Pires, I. et al. (2009) Apelin decreases myocardial injury and improves right ventricular function in monocrotaline-induced pulmonary hypertension. *Am J Physiol Heart Circ Physiol* 296 (6), H2007-2014
170 Goncalves, N. et al. (2010) A high-calorie diet attenuates cachexia and adipose tissue inflammation in monocrotaline-induced pulmonary hypertensive rats. *Rev Port Cardiol* 29 (3), 391-400
171 Yin, F.C. et al. (1982) Use of tibial length to quantify cardiac hypertrophy: application in the aging rat. *Am J Physiol* 243 (6), H941-947
172 Moreira-Rodrigues, M. et al. (2007) Cardiac remodeling and dysfunction in nephrotic syndrome. *Kidney Int* 71 (12), 1240-1248
173 Jones, J.E. et al. (2002) Serial noninvasive assessment of progressive pulmonary hypertension in a rat model. *Am J Physiol Heart Circ Physiol* 283 (1), H364-371
174 Kato, Y. et al. (2003) Progressive development of pulmonary hypertension leading to right ventricular hypertrophy assessed by echocardiography in rats. *Exp Anim* 52 (4), 285-294
175 Koskenvuo, J.W. et al. (2010) A comparison of echocardiography to invasive measurement in the evaluation of pulmonary arterial hypertension in a rat model. *Int J Cardiovasc Imaging* 26 (5), 509-518
176 Naeije, R. and Huez, S. (2007) Right ventricular function in pulmonary hypertension: physiological concepts. *European Heart Journal Supplements* 9 (H), H5-H9

177 Eysmann, S.B. et al. (1989) Two-dimensional and Doppler-echocardiographic and cardiac catheterization correlates of survival in primary pulmonary hypertension. *Circulation* 80 (2), 353-360
178 Hardziyenka, M. et al. (2006) Sequence of echocardiographic changes during development of right ventricular failure in rat. *J Am Soc Echocardiogr* 19 (10), 1272-1279
179 Nagueh, S.F. et al. (2009) Recommendations for the evaluation of left ventricular diastolic function by echocardiography. *Eur J Echocardiogr* 10 (2), 165-193
180 Schena, M. et al. (1996) Echo-Doppler evaluation of left ventricular impairment in chronic cor pulmonale. *Chest* 109 (6), 1446-1451
181 Chen, L. et al. (2001) Attenuation of compensatory right ventricular hypertrophy and heart failure following monocrotaline-induced pulmonary vascular injury by the Na+-H+ exchange inhibitor cariporide. *J Pharmacol Exp Ther* 298 (2), 469-476
182 Gomez, A. et al. (1994) Left ventricular systolic performance is depressed in chronic pulmonary emphysema in dogs. *Am J Physiol* 267 (1 Pt 2), H232-247
183 Wairiuko, G.M. et al. (2007) Stem cells improve right ventricular functional recovery after acute pressure overload and ischemia reperfusion injury. *J Surg Res* 141 (2), 241-246
184 Umar, S. et al. (2009) Allogenic stem cell therapy improves right ventricular function by improving lung pathology in rats with pulmonary hypertension. *Am J Physiol Heart Circ Physiol* 297 (5), H1606-1616
185 Molina, E.J. et al. (2009) Right ventricular effects of intracoronary delivery of mesenchymal stem cells (MSC) in an animal model of pressure overload heart failure. *Biomed Pharmacother* 63 (10), 767-772
186 Ma, D. et al. (2012) Generation of patient-specific induced pluripotent stem cell-derived cardiomyocytes as a cellular model of arrhythmogenic right ventricular cardiomyopathy. *Eur Heart J*
187 Tagawa, H. et al. (1997) Cytoskeletal mechanics in pressure-overload cardiac hypertrophy. *Circ Res* 80 (2), 281-289
188 Hidalgo, C. et al. (2009) PKC phosphorylation of titin's PEVK element: a novel and conserved pathway for modulating myocardial stiffness. *Circ Res* 105 (7), 631-638, 617 p following 638
189 Uenoyama, M. et al. (2010) Protein kinase C mRNA and protein expressions in hypobaric hypoxia-induced cardiac hypertrophy in rats. *Acta Physiol (Oxf)* 198 (4), 431-440
190 Shu, Y. et al. (2011) [The effect of 5-HD on expression of PKC-alpha in rats of chronic hypoxic pulmonary hypertension]. *Zhongguo Ying Yong Sheng Li Xue Za Zhi* 27 (3), 311-314
191 Redout, E.M. et al. (2007) Right-ventricular failure is associated with increased mitochondrial complex II activity and production of reactive oxygen species. *Cardiovasc Res* 75 (4), 770-781
192 Grutzner, A. et al. (2009) Modulation of titin-based stiffness by disulfide bonding in the cardiac titin N2-B unique sequence. *Biophys J* 97 (3), 825-834
193 Kruger, M. et al. (2008) Thyroid hormone regulates developmental titin isoform transitions via the phosphatidylinositol-3-kinase/ AKT pathway. *Circ Res* 102 (4), 439-447
194 Giraud, M.N. et al. (2005) Expressional reprogramming of survival pathways in rat cardiocytes by neuregulin-1beta. *J Appl Physiol* 99 (1), 313-322
195 Jie, B. et al. (2012) Neuregulin-1 suppresses cardiomyocyte apoptosis by activating PI3K/Akt and inhibiting mitochondrial permeability transition pore. *Mol Cell Biochem* 370 (1-2), 35-43

196 Borbely, A. et al. (2009) Transcriptional and posttranslational modifications of titin: implications for diastole. *Circ Res* 104 (1), 12-14
197 Zeng, G. et al. (2000) Roles for insulin receptor, PI3-kinase, and Akt in insulin-signaling pathways related to production of nitric oxide in human vascular endothelial cells. *Circulation* 101 (13), 1539-1545
198 Molteni, A. et al. (1984) Monocrotaline-induced pulmonary endothelial dysfunction in rats. *Proc Soc Exp Biol Med* 176 (1), 88-94
199 Sirmagul, B. et al. (2012) Assessment of the Endothelial Functions in Monocrotaline-Induced Pulmonary Hypertension. *Clin Exp Hypertens*
200 Lame, M.W. et al. (2000) Protein targets of monocrotaline pyrrole in pulmonary artery endothelial cells. *J Biol Chem* 275 (37), 29091-29099
201 Jeffery, T.K. and Wanstall, J.C. (2001) Pulmonary vascular remodeling: a target for therapeutic intervention in pulmonary hypertension. *Pharmacol Ther* 92 (1), 1-20
202 Ito, K.M. et al. (2000) Alterations of endothelium and smooth muscle function in monocrotaline-induced pulmonary hypertensive arteries. *Am J Physiol Heart Circ Physiol* 279 (4), H1786-1795
203 Peyter, A.C. et al. (2008) Muscarinic receptor M1 and phosphodiesterase 1 are key determinants in pulmonary vascular dysfunction following perinatal hypoxia in mice. *Am J Physiol Lung Cell Mol Physiol* 295 (1), L201-213
204 Orii, R. et al. (2010) M(3)muscarinic receptors mediate acetylcholine-induced pulmonary vasodilation in pulmonary hypertension. *Biosci Trends* 4 (5), 260-266
205 Hislop, A.A. et al. (1997) Endothelial nitric oxide synthase in hypoxic newborn porcine pulmonary vessels. *Arch Dis Child Fetal Neonatal Ed* 77 (1), F16-22
206 Villamor, E. et al. (1997) Chronic intrauterine pulmonary hypertension impairs endothelial nitric oxide synthase in the ovine fetus. *Am J Physiol* 272 (5 Pt 1), L1013-1020
207 Fike, C.D. et al. (1998) Chronic hypoxia decreases nitric oxide production and endothelial nitric oxide synthase in newborn pig lungs. *Am J Physiol* 274 (4 Pt 1), L517-526
208 Giaid, A. and Saleh, D. (1995) Reduced expression of endothelial nitric oxide synthase in the lungs of patients with pulmonary hypertension. *N Engl J Med* 333 (4), 214-221
209 Hironaka, E. et al. (2003) Serotonin receptor antagonist inhibits monocrotaline-induced pulmonary hypertension and prolongs survival in rats. *Cardiovasc Res* 60 (3), 692-699
210 Pei, Y. et al. (2011) Rosuvastatin attenuates monocrotaline-induced pulmonary hypertension via regulation of Akt/eNOS signaling and asymmetric dimethylarginine metabolism. *Eur J Pharmacol* 666 (1-3), 165-172
211 Murata, T. et al. (2002) Decreased endothelial nitric-oxide synthase (eNOS) activity resulting from abnormal interaction between eNOS and its regulatory proteins in hypoxia-induced pulmonary hypertension. *J Biol Chem* 277 (46), 44085-44092
212 Schermuly, R.T. et al. (2007) Phosphodiesterase 1 upregulation in pulmonary arterial hypertension: target for reverse-remodeling therapy. *Circulation* 115 (17), 2331-2339
213 Murray, F. et al. (2007) Expression and activity of cAMP phosphodiesterase isoforms in pulmonary artery smooth muscle cells from patients with pulmonary hypertension: role for PDE1. *Am J Physiol Lung Cell Mol Physiol* 292 (1), L294-303
214 Rybalkin, S.D. et al. (2003) Cyclic GMP phosphodiesterases and regulation of smooth muscle function. *Circ Res* 93 (4), 280-291

215 Lemmens, K. et al. (2007) Role of neuregulin-1/ErbB signaling in cardiovascular physiology and disease: implications for therapy of heart failure. *Circulation* 116 (8), 954-960

216 van Suylen, R.J. et al. (1998) Pulmonary artery remodeling differs in hypoxia- and monocrotaline-induced pulmonary hypertension. *Am J Respir Crit Care Med* 157 (5 Pt 1), 1423-1428

217 Abe, K. et al. (2004) Long-term treatment with a Rho-kinase inhibitor improves monocrotaline-induced fatal pulmonary hypertension in rats. *Circ Res* 94 (3), 385-393

218 Guerard, P. et al. (2006) The HMG-CoA reductase inhibitor, pravastatin, prevents the development of monocrotaline-induced pulmonary hypertension in the rat through reduction of endothelial cell apoptosis and overexpression of eNOS. *Naunyn Schmiedebergs Arch Pharmacol* 373 (6), 401-414

219 Csiszar, A. et al. (2009) Resveratrol prevents monocrotaline-induced pulmonary hypertension in rats. *Hypertension* 54 (3), 668-675

220 Yamamoto, S. (1995) Single Lung Transplantation for the Treatment of Monocrotaline-Induced Pulmonary Hypertension in the Rat. *Acta medica Nagasakiensia* 40 (1-4), 38-43

221 Hessel, M.H. et al. (2006) Characterization of right ventricular function after monocrotaline-induced pulmonary hypertension in the intact rat. *Am J Physiol Heart Circ Physiol* 291 (5), H2424-2430

222 Daicho, T. et al. (2009) Alterations in pharmacological action of the right ventricle of monocrotaline-induced pulmonary hypertensive rats. *Biol Pharm Bull* 32 (8), 1378-1384

223 Rubens, C. et al. (2001) Big endothelin-1 and endothelin-1 plasma levels are correlated with the severity of primary pulmonary hypertension. *Chest* 120 (5), 1562-1569

224 Stewart, D.J. et al. (1991) Increased plasma endothelin-1 in pulmonary hypertension: marker or mediator of disease? *Ann Intern Med* 114 (6), 464-469

225 Ichikawa, K.I. et al. (1996) Endogenous endothelin-1 mediates cardiac hypertrophy and switching of myosin heavy chain gene expression in rat ventricular myocardium. *J Am Coll Cardiol* 27 (5), 1286-1291

226 Jasmin, J.F. et al. (2003) Activation of the right ventricular endothelin (ET) system in the monocrotaline model of pulmonary hypertension: response to chronic ETA receptor blockade. *Clin Sci (Lond)* 105 (6), 647-653

227 Leuchte, H.H. et al. (2004) Clinical significance of brain natriuretic peptide in primary pulmonary hypertension. *J Am Coll Cardiol* 43 (5), 764-770

228 King, L. and Wilkins, M.R. (2002) Natriuretic peptide receptors and the heart. *Heart* 87 (4), 314-315

229 Nagaya, N. et al. (1998) Plasma brain natriuretic peptide levels increase in proportion to the extent of right ventricular dysfunction in pulmonary hypertension. *J Am Coll Cardiol* 31 (1), 202-208

230 Tirziu, D. et al. (2010) Cell communications in the heart. *Circulation* 122 (9), 928-937

231 Haworth, S.G. (2007) The cell and molecular biology of right ventricular dysfunction in pulmonary hypertension. *European Heart Journal Supplements* 9 (H), H10-H16

232 Leineweber, K. et al. (2002) Ventricular hypertrophy plus neurohumoral activation is necessary to alter the cardiac beta-adrenoceptor system in experimental heart failure. *Circ Res* 91 (11), 1056-1062

233 Ishikawa, S. et al. (1991) Biventricular down-regulation of beta-adrenergic receptors in right ventricular hypertrophy induced by monocrotaline. *Jpn Circ J* 55 (11), 1077-1085

234 de Man, F.S. et al. (2012) Dysregulated Renin-Angiotensin-aldosterone system contributes to pulmonary arterial hypertension. *Am J Respir Crit Care Med* 186 (8), 780-789

235 Morrell, N.W. et al. (1995) Angiotensin converting enzyme expression is increased in small pulmonary arteries of rats with hypoxia-induced pulmonary hypertension. *J Clin Invest* 96 (4), 1823-1833

236 Orte, C. et al. (2000) Expression of pulmonary vascular angiotensin-converting enzyme in primary and secondary plexiform pulmonary hypertension. *J Pathol* 192 (3), 379-384

237 Zisman, L.S. et al. (1998) Differential regulation of cardiac angiotensin converting enzyme binding sites and AT1 receptor density in the failing human heart. *Circulation* 98 (17), 1735-1741

238 Wang, D.L. et al. (1995) Mechanical strain increases endothelin-1 gene expression via protein kinase C pathway in human endothelial cells. *J Cell Physiol* 163 (2), 400-406

APPENDIX

The results of this master thesis were presented at several national and international scientific meetings and published in scientific journals.

Publications:

As abstracts:

Brás-Silva C, Maia-Rocha C, Mendes-Ferreira P, Adão R, Lourenço AP, Leite-Moreira AF (2011) Aumento da expressão génica de neuregulina e sua modulação pelo bosentan na hipertensão pulmonar. *Rev Port Cardiol* 30 (Supl.I): I-85

Maia-Rocha C, Mendes-Ferreira P, Adão R, Lourenço AP, Leite-Moreira AF, Brás-Silva C. (2011) Neuregulin increased expression and its modulation by bosentan in pulmonary hypertension. IJUP' 11 Abstract Book – 4th meeting of young researchers at UP, 518

Mendes-Ferreira P, Maia-Rocha C, Adão R, Silva M, Lourenço AP, Leite-Moreira AF, and Brás-Silva C. (2011) Neuregulin attenuates right ventricular hypertrophy and dysfunction in an experimental model of pulmonary hypertension. IJUP'11 Abstract Book - 4th meeting of young researchers at UP, 220.

Maia-Rocha C, Adão R, Mendes-Ferreira P, Mendes MJ, Pinho S, Lourenço AP, De Keulenaer GW, Leite-Moreira AF, Brás-Silva C. (2012) Neuregulin attenuates right ventricular hypertrophy and dysfunction in an experimental model of pulmorary hypertension. IJUP' 12 Abstract book – 5th meeting of young researchers at UP, 302

Adão R, Maia-Rocha C, Mendes-Ferreira P, Mendes MJ,Cerqueira RJ, Castro-Chaves P, De Keulenaer GW, Leite-Moreira AF, Brás-Silva C. (2012) Neuregulin attenuates pulmonary endothelial dysfunction in an experimental model of pulmorary hypertension. IJUP' 12 Abstract Book – 5th meeting of young researchers at UP, 528

Mendes-Ferreira P, Maia-Rocha C, Adao R, Lourenco AP, Cerqueira RJ, Mendes MJ, Castro-Chaves P, De Keulenaer GW, Leite-Moreira AF, Bras-Silva C. (2012) Neuregulin attenuates right ventricular hypertrophy and dysfunction in an experimental model of pulmonary hypertension. *Cardiovasc Res*, 93(1), S117

Mendes-Ferreira P, Maia-Rocha C, Adao R, Cerqueira RJ, Mendes MJ, Lourenco AP, Pinho S, De Keulenaer GW, Leite-Moreira AF, Bras-Silva C. (2012) NRG-1 improves monocrotaline-induced right ventricular and pulmonary endothelial dysfunction. *Eur J Heart Fail* Suppl 11 (suppl 1), S15-S63

As fulltext:

Lopes-Conceição L, Dias-Neto M, Fontes-Sousa AP, Mendes-Ferreira P, Maia-Rocha C, Henriques Coelho T, De Keulenaer GW, Leite-Moreira AF, Brás-Silva C. (2011) [[[Neuregulin1/ErbB system: importance in the control of cardiovascular function]. *Acta Med Port* 24 (4), 1009-1020.

Mendes-Ferreira P, De Keulenaer GW, Leite-Moreira AF, Brás-Silva C. (2012) Therapeutic potential of neuregulin-1 in cardiovascular diseases. *Drug Discov Today* (submitted).

Communications at Scientific Meetings

Oral communications:

Mendes-Ferreira P, Maia-Rocha C, Adão R, Silva M, Lourenço AP, Leite-Moreira AF, and Brás-Silva C. Neuregulin attenuates right ventricular hypertrophy and dysfunction in an experimental model of pulmonary hypertension. IJUP'11 - 4th meeting of young researchers at Uiversity of Porto. 17-19 February, 2011. Porto, Portugal.

Brás-Silva C, Fontes–Sousa AP, Almeida M, Pinho S, Moura C, Pires A, Areias JC (Mendes-Ferreira P, Maia-Rocha C, Adão R, Silva M, Mendes MJ, Lourenço AP, Leite-Moreira AF). Bolsa de Estudo João Porto - O papel do sistema da neuregulina na fisiopatologia da hipertensão pulmonar e na progressão para a insuficiência cardíaca. XXXII Congresso Português de Cardiologia. 8-10 de Abril, 2011. Lisboa, Portugal.

Maia-Rocha C, Adão R, Mendes-Ferreira P, Mendes MJ, Pinho S, Lourenço AP, De Keulenaer GW, Leite-Moreira AF, Brás-Silva C. Neuregulin attenuates right ventricular hypertrophy and dysfunction in an experimental model of pulmorary hypertension IJUP' 12 – 5th meeting of youngresearchers at University of Porto. 2012: A1. on 22,23 and 24 February 2012

Mendes-Ferreira P, Maia-Rocha C, Adao R, Lourenco AP, De Keulenaer GW, Leite-Moreira AF, Brás-Silva C. A neuregulina atenua a hipertrofia e a disfunção ventricular direitas num modelo experimental de hipertensão pulmonar. XXXIII Congresso Português de Cardiologia. 22nd-24th April, 2012. Vilamoura, Portugal. (Finalista do Prémio Melhor Comunicação Oral)

Mendes-Ferreira P, Adão R, Cerqueira RJ, Maia-Rocha C, Mendes MJ, Castro-Chaves P, De Keulenaer GW, Leite-Moreira AF, Brás-Silva C. A neuregulina-1 atenua a disfunção endotelial na hipertensão arterial pulmonar. XXXIII Congresso Português de Cardiologia. 22nd-24th April, 2012. Vilamoura, Portugal. (Finalista do Prémio Jovem Investigardor - Investigação Básica)

Mendes-Ferreira P, Maia-Rocha C, Adao R, Lourenco AP, Moura C, Pinho S, Areias JC, De Keulenaer GW, Leite-Moreira AF, Bras-Silva C. NRG-1 improves right ventricular function in pulmonary hypertension. European Congress of Cardiology. 25-29 August. Munich. Germany.

Mendes-Ferreira P, Adão R, Maia-Rocha C, Cerqueira RJ, Mendes MJ, Castro-Chaves P, De Keulenaer GW, Leite-Moreira AF, Brás-Silva C. Neuregulin attenuates pulmonary endothelial dysfunction in pulmonary hypertension. European Congress of Cardiology. 25-29 August. Munich. Germany.

Poster communications:

Maia-Rocha C, Mendes-Ferreira P, Adão R, Lourenço AP, Leite-Moreira AF, and Brás-Silva C. Neuregulin increased expression and its modulation by bosentan in pulmonary hypertension. IJUP'11 - 4th meeting of young researchers at Uiversity of Porto. 17-19 February, 2011. Porto, Portugal.

Brás-Silva C, Maia-Rocha C, Mendes-Ferreira P, Adão R, Lourenço AP, Leite-Moreira AF. Aumento da expressão génica de neuregulina e sua modulação pelo bosentan na hipertensão pulmonar. XXXII Congresso Português de Cardiologia. 8-10 de Abril, 2011. Lisboa, Portugal.

Mendes-Ferreira P, Maia-Rocha C, Adao R, Lourenco AP, Cerqueira RJ, Mendes MJ, Castro-Chaves P, De Keulenaer GW, Leite-Moreira AF, Bras-Silva C. Neuregulin attenuates right ventricular hypertrophy and dysfunction in an experimental model of pulmonary hypertension. YES Meeting 2011 - Young European Scientist Meeting. 16th - 18th September, 2011. Porto, Portugal.

Adão R, Maia-Rocha C, Mendes-Ferreira P, Mendes MJ,Cerqueira RJ, Castro-Chaves P, De Keulenaer GW, Leite-Moreira AF, Brás-Silva C. Neuregulin attenuates pulmonary endothelial dysfunction in an experimental model of pulmorary hypertension. IJUP' 12 – 5th meeting of youngresearchers at University of Porto. 2012: on 22,23 and 24 February 2012.

Mendes-Ferreira P, Maia-Rocha C, Adao R, Lourenco AP, Cerqueira RJ, Mendes MJ, Castro-Chaves P, De Keulenaer GW, Leite-Moreira AF, Bras-Silva C. Bras-Silva. Neuregulin attenuates right ventricular hypertrophy and dysfunction in an experimental model of pulmonary hypertension. Frontiers in Cardiovascular Biology, 30th March - 1st April, London, United Kingdon.

P. Mendes-Ferreira, C. Maia-Rocha, R. Adao, RJ. Cerqueira, MJ. Mendes, AP. Lourenco, S. Pinho, GW. De Keulenaer, AF. Leite-Moreira, C. Bras-Silva. NRG-1 improves monocrotaline-induced right ventricular and pulmonary endothelial dysfunction. Heart Failure Congress 2012. 19th – 22nd May 2012. Belgrade – Serbia.

Mendes-Ferreira P, Maia-Rocha C, Adao R, Cerqueira RJ, Mendes MJ, Lourenço AP, De Keulenaer GW, Leite-Moreira AF, Bras-Silva C. Neuregulin Attenuates Right Ventricular and Pulmonary Endothelial Dysfunction in an Experimental Model of Pulmonary Hypertension. American Heart Association, Scientific Sessions 2012. 3rd – 7th November 2012. Los Angeles, California, United States of America.

Mendes-Ferreira P, Maia-Rocha C, Adao R, Cerqueira RJ, Mendes MJ, Lourenço AP, De Keulenaer GW, Leite-Moreira AF, Bras-Silva C. Bras-Silva. Neuregulin Attenuates Right Ventricular and Pulmonary Endothelial Dysfunction in an Experimental Model of Pulmonary Hypertension. 5h World Symposium on Pulmonary Hypertension. 27th February – 1st March 2012. Nice, France (accepted for presentation).